From the Department of Clinical Neuroscience,
Karolinska Institutet, Stockholm, Sweden

ELECTROPHYSIOLOGY-BASED INVESTIGATIONS OF G PROTEIN-COUPLED RECEPTOR PHARMACOLOGY

Richard Ågren

Karolinska Institutet

Stockholm 2020

All previously published papers were reproduced with permission from the publisher.
Published by Karolinska Institutet.
Printed by US-AB, 2020
© Richard Ågren, 2020
ISBN 978-91-7831-816-2

ELECTROPHYSIOLOGY-BASED INVESTIGATIONS OF G PROTEIN-COUPLED RECEPTOR PHARMACOLOGY

THESIS FOR DOCTORAL DEGREE (Ph.D.)

Public defense at Torsten N Wiesel lecture hall, J3:04, Karolinska University Hospital, Solna
Friday 15th of May at 13.00 p.m.

By

Richard Ågren

Principal Supervisor:
Dr. Johanna Nilsson
Karolinska Institutet
Department of Clinical Neuroscience
Örebro University
Department of Medical Sciences

Co-supervisors:
Professor Peter Århem
Karolinska Institutet
Department of Neuroscience

Dr. Kristoffer Sahlholm
Umeå University
Department of Integrative Medical Biology
Karolinska Institutet
Department of Neuroscience

Opponent:
Professor Bernhard Bettler
University of Basel
Department of Biomedicine

Examination Board:
Dr. Kent Jardemark
Karolinska Institutet
Department of Physiology and Pharmacology

Professor Lars Farde
Karolinska Institutet
Department of Clinical Neuroscience

Professor Bryndis Birnir
Uppsala University
Department of Medical Cell Biology

ABSTRACT

G protein-coupled receptors (GPCRs) constitute targets for ~34% of approved drugs. The muscarinic acetylcholine M_2 receptor (M_2R) activates G protein-coupled receptor inward rectifying potassium (GIRK) channels in the central nervous system and heart. Membrane potential modulates agonist potency at several GPCRs. However, the mechanism underlying the voltage sensitivity remains debated. A highly conserved aspartate residue ($D^{2.50}69$) has been proposed to mediate the voltage-sensitivity of the M_2R, although the low expression of D69 mutants has complicated further functional investigations.

Dopamine D_2 and D_3 receptors (D_2R and D_3R) are pre- and postsynaptic inhibitory receptors in the central nervous system, involved in locomotion, cognition and endocrine functions. D_2R antagonists and weak partial agonists are used clinically as antipsychotics but are associated with several side effects. Various strategies have been suggested to reduce the side-effect profile of novel antipsychotic drugs. One such strategy includes the selective targeting of non-canonical signaling pathways, e.g., the β-arrestin pathway, while leaving the classical, G protein pathway, undisturbed. Additionally, binding affinity and kinetics at the D_2R, as well as ligand lipophilicity, have been suggested to be of significance in determining the side-effect liability of antipsychotics.

In the thesis, M_2R, D_2R and D_3R were investigated using two-electrode voltage-clamp in *Xenopus laevis* oocytes co-expressing the respective receptor and GIRK channels. M_2R carrying a charge-neutralizing D69N mutation demonstrated a voltage-dependent shift of agonist-potency, similar to the wild type M_2R. This finding is in line with a recent alternative hypothesis, which implicates three tyrosine residues in the M_2R voltage sensor. The proposed β-arrestin-selective partial D_2R agonist, UNC9994, was found to be a weak partial- and almost full agonist at D_2R and D_3R mediated GIRK activation, respectively. These findings are incongruent with β-arrestin-selectivity and suggest that the promising effects of UNC9994 in animal models of psychosis may be related, at least in part, to involvement of the D_3R. Finally, the partial D_2R agonist positron emission tomography ligand, SV-III-130, demonstrated an insurmountable, yet competitive, binding mechanism at the D_2R. Mutations of residues in a secondary binding pocket, engaging the secondary pharmacophore, abolished the insurmountable binding. Kinetic models incorporating an irreversible, SV-III-130-bound state captured the experimentally observed data. Molecular dynamics simulations suggested that D_2R extracellular linkers participate in an induced-fit binding mechanism.

In summary, the thesis addresses the mechanism of voltage-dependent agonist-potency at GPCRs and contradicts earlier reports of a β-arrestin-selective action of the experimental antipsychotic, UNC9994, at the D_2R. Finally, a two-step induced-fit binding mechanism was demonstrated for the aripiprazole analogue, SV-III-130, at the D_2R. The findings may guide further mechanistic investigations and provide insights for the development of novel diagnostic and therapeutic GPCR ligands.

LIST OF SCIENTIFIC PAPERS INCLUDED IN THE THESIS

I. **Ågren R**, Sahlholm K, Nilsson J, Århem P. Point mutation of a conserved aspartate, D69, in the muscarinic M2 receptor does not modify voltage-sensitive agonist potency. Biochem Biophys Res Commun. 2018 Jan 29;496(1):101-104.

II. **Ågren R**, Århem P, Nilsson J*, Sahlholm K*. The Beta-Arrestin-Biased Dopamine D2 Receptor Ligand, UNC9994, Is a Partial Agonist at G-Protein-Mediated Potassium Channel Activation. Int J Neuropsychopharmacol. 2018 Dec 1;21(12):1102-1108.

III. **Ågren R**, Zeberg H, Stepnięwski TM, Reilly SW, Luedtke R, Århem P, Mach RH, Selent J, Nilsson J, Sahlholm K. A ligand with two modes of interaction with the dopamine D2 receptor – An induced-fit mechanism of irreversible binding (manuscript)

* Equal contributions

SCIENTIFIC PAPER NOT INCLUDED IN THE THESIS

Ågren R, Nilsson J, Århem P. Closed and open state dependent block of potassium channels cause opposing effects on excitability - a computational approach. Sci Rep. 2019 Jun 3;9(1):8175.

TABLE OF CONTENTS

LIST OF ABBREVIATIONS

5-HT_{1-7}R	Serotonin 1-7 receptors
AT_1R	Angiotensin II type 1 receptor
cAMP	Cyclic adenosine monophosphate
D_{1-5}R	Dopamine D_{1-5} receptors
EC_{50}	Half maximal effective concentration
ECL1-3	Extracellular loops 1-3
E_{max}	Intrinsic activity
EPS	Extrapyramidal symptoms
ERK1	Extracellular signal-related kinase 1
HEPES	4-(2-hydroxyethyl)-1-piperazineethanesulfonic acid
$GABA_{B1-2}$R	Metabotropic γ-aminobutyric acid receptor, subunits 1-2
GAP	Guanosine triphosphatase accelerating proteins
GPCR	G protein-coupled receptor
GIRK	G protein-coupled inward rectifier potassium channel
GDP	Guanosine diphosphate
GTP	Guanosine triphosphate
GRK2	G protein-coupled receptor kinase 2
GSK3β	Glycogen synthase kinase 3β
IC_{50}	Half maximal inhibitory concentration
IP_3	Inositol 1,4,5-trisphosphate
K_d	Dissociation constant
K_i	Inhibition constant
k_{obs}	Observed association rate
k_{off}	Dissociation rate constant
k_{on}	Association rate constant
M_{1-5}R	Muscarinic acetylcholine M_{1-5} receptors
$mGlu_{1-3}$R	Metabotropic glutamate receptors 1-3
MS-222	Tricaine methanesulfonate
NMDA	N-methyl-D-aspartate
μ-OR	μ-Opioid receptor

OBP	Orthosteric binding pocket
PCP	Phencyclidine
PET	Positron emission tomography
PIP_2	Phosphatidylinositol 4,5-bisphosphate
PKB	Protein kinase B
PTX	Pertussis toxin
PTX-S1	Catalytic subunit of pertussis toxin
PPHT	2-(N-phenethyl-N-propyl)amino-5-hydroxytetralin
RGS	Regulator of G protein signaling
SBP	Secondary binding pocket
TEVC	Two-electrode voltage-clamp
WT	Wild type

1 INTRODUCTION

1.1 G-PROTEIN COUPLED RECEPTORS

During the 20th century, theories of receptor-ligand interactions were derived from experiments on myocytes and glands. In 1972, the β-adrenergic G-protein coupled receptor (GPCR) was identified and purified by Lefkowitz et al. (1). This was followed by structural determination of the photon-sensitive visual rhodopsin, and later cloning of the β2 adrenergic receptor (2). GPCRs, consisting of seven transmembrane helices, enable transmission and amplification of extracellular factors to intracellular signals by canonical, i.e., G-protein, and non-canonical, e.g., β-arrestin, pathways. The widespread expression of GPCRs in a multitude of cells and their involvement in disease support pharmacological targeting; currently 34% of all approved drugs target GPCRs (3).

1.2 DIMENSIONS OF RECEPTOR PHARMACOLOGY

Physiological, or pathological, receptor expression *in vivo* determines the target area of a receptor ligand. GPCRs involved in the modulation of neuronal signaling typically span the cell membrane and are located either pre- and/or postsynaptically. The ligand may either target one specific type of receptor (receptor-specific), mainly prefer one type of receptor (receptor-preferring) or target a whole span of different receptors (multireceptor, or "dirty", targeting) (Fig. 1A). Most clinically used GPCR ligands interact with several receptors. For example, most antipsychotic drugs bind to dopamine, but also to serotonin, α-adrenergic, muscarinic acetylcholine and histaminergic receptors, each interaction associating with different clinical (side-)effects (see e.g. (4)).

Receptors may exist as monomers, homomers or heteromers, and only signal as obligate heteromers (Fig. 1B). This was first demonstrated for the G protein-coupled γ-aminobutyric acid receptor ($GABA_BR$), which requires co-expression of $GABA_{B1}R$ subunits with $GABA_{B2}R$ subunits to form functional receptors (5). Based on the assumption that heteromers are selectively expressed in regions of interest, ligands targeting specific heteromers may reduce the degree of side-effects (6).

When the ligand is in the vicinity of a targeted receptor, the probability of a binding event occurring is dependent on the ligand concentration (L), the receptor concentration (R), the ligand association rate constant (k_{on}) and the ligand dissociation rate constant (k_{off}),

$$R + L \underset{k_{off}}{\overset{k_{on}}{\rightleftharpoons}} RL$$

where RL is the ligand-bound receptor (Fig. 1C). Assuming a one-step binding mechanism, the binding rate constants dictate the dissociation constant (K_d; k_{off}/k_{on}). Both association and dissociation rate constants are critically dependent on the amino acid residues in the access pathway to the receptor binding site. An example illustrating the role of the first extracellular loop (ECL1) in regulating ligand entry and egress was illustrated by increased association and

dissociation rates of the antipsychotic drug risperidone at the dopamine D_2 receptor (D_2R) following mutation of W100 (7).

Typically, the ligands bind to amino acid residues in one or several receptor cavities, either by a single- or a multistep-process, respectively. An example of the latter is heterobivalent ligand binding (8); illustrated by a ligand composed of two (primary and secondary) pharmacophores, i.e. ligand fragments with affinities to macromolecules, which bind with different affinities to two distinct receptor sites (the primary or orthosteric binding pocket; OBP and the secondary binding pocket; SBP) respectively (Fig. 1D). The endogenous ligand typically binds to the OBP, activating the receptor. Depending on the affinities of the two pharmacophores to the OBP and SBP respectively, two different heterobivalent binding modes are possible; high affinity of the primary pharmacophore to the OBP would allow for an "abII" binding mode, whereas a high affinity of the secondary pharmacophore to the SBP would facilitate an "abI" binding mode (8)(illustrated in Fig. 1D).

Induced-fit binding is another multistep mechanism, where the ligand primary pharmacophore first binds to the OBP causing a conformational rearrangement of the receptor, which allows for subsequent binding of the secondary pharmacophore to the SBP (9)(illustrated in Fig. 1E). Such induced-fit binding may entail a prolonged drug residence time *in vivo* (10).

The receptor-bound ligand may elicit a spectrum of responses depending on its intrinsic activity (E_{max}; Fig. 1F). An agonist could demonstrate supramaximal, full or partial efficacy; different amplitudes of responses, as compared to the response evoked by a reference full agonist (typically the endogenous ligand). A neutral antagonist has no efficacy and rather competes with agonists to abolish the response. Several antipsychotic drugs demonstrate partial agonist or antagonist features at the D_2R, while antagonizing serotonin 2 receptors (5-HT_2Rs) (11). In addition, inverse agonists reduce the constitutive receptor activity; i.e., inhibit the background signaling of the receptor in the absence of an agonist. β-blockers demonstrating inverse agonism, e.g. propranolol, act at β-adrenergic receptors in the heart and skeletal muscles, and are used to reduce tachycardia and essential tremor (12, 13).

Allosteric GPCR ligands may interact with separate, allosteric binding sites to modulate both the affinity and efficacy of ligands at the OBP (14, 15). For the $GABA_BR$, CGP7930 was one of the first reported positive allosteric modulators (16). Allosteric GPCRs modulators may affect endogenous ligand-receptor interactions only subtly, thereby allowing for additional strategies of targeting a range of conditions, including e.g. inflammation, psychosis, addiction and nociception (see (17)).

At the signaling level, a ligand could activate any of the various G protein subtypes, e.g. $G\alpha_s$, $G\alpha_i$, $G\alpha_o$, $G\alpha_q$, G_z, G_{olf}, $G\alpha_{12/13}$, or the non-canonical β-arrestin pathway, with differential efficacies (Fig. 1G). Agonist-dependent G protein signaling bias has been demonstrated *in vitro* (18). Biased-signaling ligands, i.e. ligands preferentially activating either G protein or β-arrestin pathways, may be of importance in reducing side-effects and potentiating therapeutic

drug effects. Oliceridine is a G protein-biased μ-opioid receptor (μ-OR) agonist that has been suggested to reduce constipation and respiratory depression, while maintaining the antinociceptive effect (19).

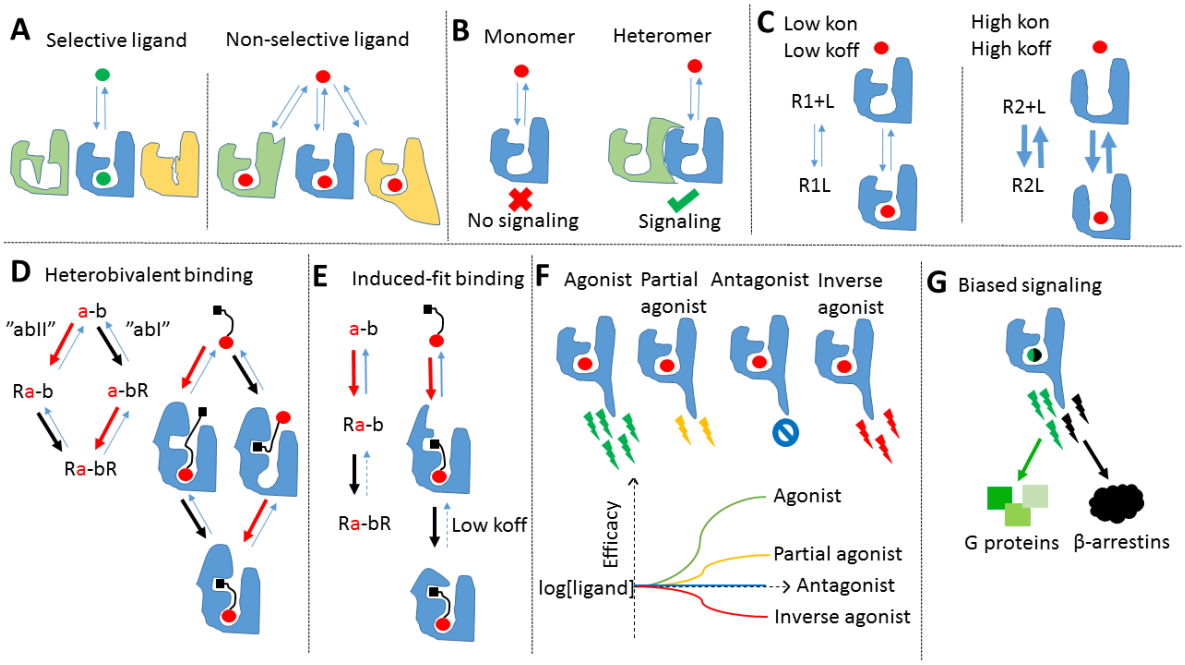

Figure 1. Summary of key dimensions of receptor-ligand interaction. A) Receptor selectivity. Left, the selective ligand (green) only binds to one receptor (blue). Right, the non-selective ligand (red) binds to all receptors. B) Heteromer-dependent signaling. Left, ligand binding to the monomer does not evoke a response. Right, ligand binding to the heteromer evokes a response. C) Association and dissociation rate constants dictate the dissociation constant K_d. Note that the K_d ratio could be identical for the low k_{off}/low k_{on} and the high k_{off}/high k_{on} examples. D) Heterobivalent ligand binding, with primary (a) and secondary (b) pharmacophores of a bitopic ligand (a-b) interacting with two distinct receptor binding sites; the OBP and the SBP respectively. Mechanistically, either the secondary (black arrow) or the primary pharmacophore (red arrow) may bind the receptor first, described as abI- and abII-mechanisms respectively (8). E) Induced-fit binding is viewed as an initial binding event between the primary pharmacophore (a) and the OBP (red arrow), followed by a conformational change allowing binding of the secondary pharmacophore (b) to the SBP (9)(black arrow). Note that the latter event reverses only slowly (low k_{off}). F) Agonist efficacy (or intrinsic activity). Following receptor-ligand interaction, the downstream signaling is fully induced by an agonist (green), partially induced by a partial agonist (yellow), abolished by an antagonist (blue) and reduced below the baseline (constitutive) level by an inverse agonist (red). G) Biased signaling. The ligand activates both G protein (green) and β-arrestin signaling pathways (black). Details are not drawn to scale.

1.3 G PROTEIN-SIGNALING PATHWAYS

1.3.1 Activation of G protein signaling pathways

GPCRs are recognized by their ability to induce G protein mediated signaling following activation. Ligand-activated GPCRs gain guanine-nucleotide exchange factor (GEF) properties, releasing guanosine diphosphate (GDP) from heterotrimeric G protein complexes of GαGDP/Gβγ (see (20)). This promotes binding of guanosine triphosphate (GTP) to Gα, inducing an activating conformational change, and possibly separating the Gα and Gβγ proteins (21). Depending on the G protein subtype, i.e. $G\alpha_s$ or $G\alpha_i$/$G\alpha_o$, GαGTP stimulates or

inhibits adenylate cyclase (AC) which converts ATP into 3',5'-cyclic AMP (cAMP). The Gα protein stimulating AC, $G\alpha_s$, may be ADP-ribosylated and activated by the *V. Cholera* toxin (22, 23), whereas the AC inhibitory $G\alpha_i/G\alpha_o$ proteins may be ADP-ribosylated and inactivated by the *B. pertussis* toxin (PTX)(24, 25). Historically, this has facilitated the isolation and study of selected Gα proteins. Downstream of the GPCR, cAMP binds to, and activates protein kinase A, in turn phosphorylating the cAMP-response element binding protein, which binds to genomic cAMP response elements and induces transcription. Also, cAMP may directly activate cyclic-nucleotide gated channels (26). In similar, Gβγ proteins modulate ion channel activities, e.g. of L- and T-type voltage-gated calcium channels, and activate G protein-coupled inward rectifying potassium 1-4 (GIRK1-4) channels (27, 28).

1.3.2 G protein-coupled inward rectifying potassium channels

GIRK1-4 are expressed in the central nervous system and contribute to neuronal hyperpolarization (29, 30). Functional channels consist of GIRK1-4 subunit heterotetramers (with exception of GIRK2; able to form homotetramers), each consisting of two transmembrane helices (30, 31). For GIRK channel activation, phosphatidylinositol 4,5-bisphosphate (PIP_2) is required in addition to Gβγ (32). Also, GIRK channels are modulated by sodium ions, which might serve as a mechanism to hyperpolarize the cell following depolarization-induced sodium influx (33, 34). The specificity between G protein and GIRK channel activation is believed to be due to the higher rate of G protein activation, and thereby Gβγ generation, by $G\alpha_i/G\alpha_o$-coupled receptors as compared to G_q- and G_s-coupled receptors (35).

1.3.3 Termination of the G protein signaling cascade

Signal termination is evoked by the GTPase activity intrinsic to Gα proteins, hydrolyzing GTP into GDP and subsequently releasing inorganic phosphate. This is followed by sequestration of Gβγ proteins, which reform with Gα proteins. By stabilization, GTPase accelerating proteins (GAPs), including the regulator of G protein signaling (RGS) family, augment the catalytic activity of the Gα GTPase domain and thereby decrease the life time of the active, GTP-bound complex (see (20)). Structurally, the RGS domain consists of nine α-helices, although there are functional differences between the GAPs; e.g. RGS4, being pre-coupled to GIRK1/2 channels, potently accelerates G protein dependent gating, whereas the free cytosolic RGS3 only accelerates G protein dependent gating with 100-fold lower potency (36). Beyond modulation of AC by $G\alpha_s$ and $G\alpha_i/G\alpha_o$ pathways, the $G\alpha_q$ protein activates phospholipase Cβ, hydrolyzing PIP_2 to diacylglycerol and inositol 1,4,5-trisphosphate (IP_3). Following activation of the IP_3 receptor, located in the membrane of the endoplasmatic reticulum, Ca^{2+} is released to the cytosol, inducing transcriptional effects through Ca^{2+}/calmodulin-dependent protein kinase II. Furthermore, a diverse array of G proteins have been characterized with a multitude of functions; e.g. activation of $G\alpha_{12/13}$ proteins have been related to cell structure functions, e.g. actin remodeling (37). Finally, the differential activation of G proteins, and the kinetics within the signaling pathways, vary between GPCRs (18).

1.4 NON-CANONICAL GPCR SIGNALING BY BETA-ARRESTINS

Active GPCRs recruit GPCR kinases, e.g. GPCR kinase 2 (GRK2), responsible for GPCR phosphorylation and signal termination. GPCR phosphorylation enhances the recruitment of β-arrestin 1 and 2 to the GPCR, which induces GPCR desensitization (see (38)). In addition, β-arrestins activate downstream signaling pathways, separate from those activated by G-proteins, e.g. nuclear factor kappa-light-chain-enhancer of activated B cells and tumor suppressor protein p53, regulating cell metabolism, mitochondrial function and synaptic plasticity in neurons (39-41). In addition, both G protein and β-arrestin signaling activate the extracellular signal-related kinase 1 (ERK1) pathway albeit with different kinetics; the former induces a rapid activation and deactivation, whereas the latter induces a slow activation and prolonged response (42, 43). Also, the β-arrestin-activated ERK1 remains cytoplasmic, as compared to the G protein-induced ERK1, which translocates to the nucleus (42, 43). G protein-independence of β-arrestin downstream signaling has been proposed (44, 45), although an investigation using mammalian cell lines with genetically deleted $G\alpha_s/G\alpha_q/G\alpha_{12}$ in conjunction with the $G\alpha_{i/o}$-inactivating PTX demonstrated G protein-dependence of β-arrestin signaling through ERK1 (46).

Antipsychotic effects of D_2R antagonists have been related to β-arrestin signaling, whereas extrapyramidal symptoms (EPS; i.e. dystonia, akathisia, tremor and tardive dyskinesia) have been suggested to result from interference with G protein signaling (45, 47). The mood stabilizer lithium has been proposed to inhibit glycogen synthase kinase 3β (GSK3β) signaling via modulation of a signaling complex consisting of β-arrestin, protein phosphatase 2A and protein kinase B (PKB) (44). At cardiomyocyte angiotensin II type 1 receptors (AT_1R), activation of β-arrestin signaling conferred positive inotropic effects, although these were counteracted by G protein-signaling activation (48). Thus, further development of β-arrestin-selective AT_1R and D_2R ligands for cardiac failure and schizophrenia may prove valuable. In contrast, at the μ-OR, G protein signaling was related to analgesic effects, whereas β-arrestin signaling was related to gastrointestinal and respiratory adverse effects (19).

1.5 MUSCARINIC ACETYLCHOLINE RECEPTORS

Acetylcholine is the endogenous agonist at metabotropic muscarinic acetylcholine $M_{1\text{-}5}$ receptors ($M_{1\text{-}5}R$), which are structurally highly homologous, but differ in G protein signaling; M_1R, M_3R and M_5R activate $G\alpha_q$, whereas M_2R and M_4R activate $G\alpha_i$, (49). $M_{1\text{-}5}R$ are expressed in the peripheral and central nervous system in varying degrees (see (50) for review). M_1R is expressed in the cortex and the striatum, and is involved in regulating dopamine release from substantia nigra. $M_1R^{-/-}$ mice display basal and amphetamine-induced hyperlocomotion as compared to wild type (WT) mice (51)). M_2R and M_3R are involved in parasympathetic nervous system responses (52). For example, cardiac acetylcholine release, which induces M_2R activation, $G\beta\gamma$ release and subsequent GIRK channel activation, contributes to membrane repolarization and a negative chronotropic effect (53). The inhibitory M_4R is present in cholinergic interneurons in the striatum, reducing dopaminergic tone and inhibiting movement (54). For hypodopaminergic conditions, e.g. Parkinson's disease, pharmacological inhibition of the M_4R may prove valuable (55). The M_5R is expressed in dopaminergic neurons in the substantia nigra and ventral tegmental area, and has

been suggested involved in opioid reward; $M_5R^{-/-}$ mice displayed reduced reward from morphine administration (56). Although high degrees of homology between the $M_{1\text{-}5}R$ have complicated the development of receptor subtype-specific ligands, recently reported crystal structures of M_1R and M_4R (57), M_2R (58), M_3R (59) and M_5R (60) will likely facilitate *in silico* ligand development.

1.6 VOLTAGE-SENSITIVITY OF GPCRS

Voltage-gated and, to some extent, ligand-gated ion channels functionally depend on voltage-sensitivity (61). Interestingly, in 2003, also GPCRs were demonstrated to be voltage-sensitive; acetylcholine potency at the M_2R was reduced at depolarized potentials in GIRK activation- and radioligand binding assays (62). In contrast, the M_1R was found to possess an inverse voltage-dependence, binding acetylcholine with increased affinity at depolarized potentials (62). Experiments on metabotropic glutamate 1-3 receptors ($mGlu_{1\text{-}3}R$) revealed differential voltage-dependent agonist potencies. Following depolarization, glutamate potency at the $G\alpha_q$-coupled $mGlu_1R$ increased, whereas glutamate potency decreased at the $G\alpha_i$-coupled $mGlu_3R$ (63). In search of a voltage-sensor, gating-charges were recorded in the M_2R, and were consistent with the voltage-sensitivity of ligand binding (64). The voltage-sensitivity of ligand potency was subsequently demonstrated in D_2R, histamine H3 and H4 receptors, generalizing the concept to include numerous GPCRs (65-67). Further investigations revealed ligand-specificity of the voltage-dependent shift in agonist potency at the D_2R; in contrast to aporphines, which retained potency and efficacy at -80 mV and at 0 mV, several other D_2R agonists demonstrated reduced potencies and, for some agonists, also reduced E_{max} at depolarized potentials (68).

In search for the GPCR voltage-sensor(s), a well-conserved aspartate residue, $D^{2.50}69$ (Ballesteros-Weinstein nomenclature; (69)), was proposed to confer the voltage-sensing properties of the M_2R, as D69 is involved in coordinating a charged sodium ion within the seven transmembrane helices (70). M_2R D69A demonstrated no gating currents, although surface expression of the mutant receptor was reduced (71). Additional investigations, based on molecular dynamics simulations, supported the role of the D69 residue in regulating M_2R voltage-sensitivity (72). Recently, tyrosine-phenylalanine substitution of three residues ($Y^{3.33}104$, $Y^{6.51}403$ and $Y^{7.39}426$) surrounding the OBP, were demonstrated to eliminate the voltage-dependent agonist potency (73). However, the involvement of the $D^{2.50}69$ in the voltage-sensing of the M_2R, and other GPCRs, still remains unclear.

The voltage-dependent agonist potency at GPCRs explains a cardiac phenomenon; the depolarization-induced decrease of acetylcholine-dependent potassium current in sinoatrial node cardiomyocytes (74). Based on electrophysiological investigations of atrial cardiomyocytes, this finding is mechanistically related to the lower potency of acetylcholine at M_2R in depolarized cells (75).

1.7 DOPAMINE RECEPTORS

In the 1950s, Arvid Carlsson discovered the ability of dopamine to reverse loss of motor functions following reserpine-induced depletion of synaptic vesicles (see (76) for an overview). This finding distinguished dopamine from the related monoamine serotonin and paved the way for understanding the role of dopamine in modulating cognition, mood,

learning, memory, motor and endocrine functions (77, 78). Dopamine receptors are classified by their main signaling pathways; D_1-like receptors (D_1R and D_5R) activate stimulatory $G\alpha_{s/olf}$ and D_2-like receptors (D_2R, D_3R and D_4R) activate inhibitory $G\alpha_{i/o}$ proteins (79). The regional expression of dopamine receptors differs; postmortem autoradiography studies indicated high expression levels of D_1R and D_2R in the caudate nucleus and putamen, with D_1R concentrated to the medial caudate nucleus in contrast to the more evenly distributed D_2R (80). Additionally, D_1R, more densely expressed in cortical regions as compared to D_2R (80), has been related to physiological and pathological cognitive functioning (81-83). D_1R is mainly postsynaptically expressed, in contrast to D_2R, which is present both pre- and postsynaptically (77). Prominent heterodimerization of dopamine receptors, e.g. D_1R-D_3R, D_1R-D_2R, and D_2R-D_3R provides additional complexity to receptor subgroup signaling (84, 85). The reported crystal structures of D_2-like receptors; D_2R (7), D_3R (86) and D_4R (87), allow for *in silico* design of selective ligands.

Dopaminergic signaling is mediated by three separate pathways, the nigrostriatal, the mesocorticolimbic and the tuberoinfundibular pathway (see (88) for review). Briefly, the nigrostriatal pathway consists of dopamine neurons in substantia nigra pars compacta projecting to the caudate nucleus and putamen, modulating motor functions but also memory, and to some extent reward. The mesocortical and mesolimbic pathways consist of dopamine neurons in the ventral tegmental area projecting to the cortex, modulating executive functions, and to the nucleus accumbens, mediating reward and positive reinforcement. The tuberoinfundibular pathway consists of dopamine neurons of the hypothalamic arcuate nucleus projecting to the hypophysis.

1.8 DOPAMINE RECEPTORS AS TARGETS

1.8.1 Dopaminergic disorders

Numerous pathological conditions, e.g. Parkinson's disease, hyperprolactinemia, Huntington's disease, schizophrenia, bipolar disorder and addiction are related to hypo- or hyperactive dopaminergic signaling (89-94). For schizophrenia, the dopamine hypothesis has been revised multiple times. Hyperactive mesolimbic dopamine signaling has been proposed to be responsible for positive symptoms (hallucinations, delusions and thought disorder) while hypoactive mesocortical dopamine signaling would explain negative (flattened affect, avolition, alogia) and cognitive symptoms (95). Accumulating evidence from neuroimaging, genome-wide association- and epidemiological studies has updated the dopamine hypothesis. Genetic variants and mutations are thought to drive a presynaptic increase in dopamine levels, which increase the probability of developing psychotic disorders, including schizophrenia, and to disturb the perception of external stimuli (96). An alternative hypothesis of schizophrenia, glutamatergic dysregulation, was based on N-methyl-D-aspartate (NMDA)-antagonists, e.g. phencyclidine (PCP) and ketamine, replicating the positive, negative, and cognitive symptoms seen in schizophrenia (97). Finally, the kynurenine hypothesis involves glutamatergic dysregulation related to increased concentrations of kynurenic acid, an endogenous NMDA-antagonist, in patients with schizophrenia (98).

1.8.2 Clinically used antipsychotics

The mainstay of pharmacological treatment of schizophrenia is currently D_2R blockade, by antagonists, or weak partial agonists. First-generation or typical antipsychotic drugs, based on the first agent chlorpromazine discovered in 1952, are recognized as ligands with high D_2R potency, prone to evoke EPS at high concentrations (99). In positron emission tomography (PET) studies of schizophrenic patients treated with typical antipsychotic drugs, the D_2R occupancy was 70-89%, with higher receptor occupancy related to EPS (100). This seemingly narrow therapeutic interval stimulated investigations to explain- and decrease the EPS propensity of antipsychotic drugs. The second-generation or atypical antipsychotics, initially based on clozapine (first discovered in 1958), demonstrated reduced EPS propensities (101). The typical/atypical drug classification has been questioned, as this classification does not fully explain the EPS frequency (102). In addition, third-generation antipsychotics refer to drugs demonstrating partial D_2R agonism, e.g. aripiprazole, and more recently also brexpiprazole, cariprazine and lumateperone (103). Due to more pronounced presynaptic D_2R receptor reserves, a partial agonist may activate autoreceptors to a larger extent than postsynaptic receptors, thereby decreasing dopamine synthesis and release (103). Alternatively, assuming increased synaptic dopamine concentrations in the mesolimbic pathway, partial agonists may functionally antagonize D_2Rs, based on their low E_{max}. Oppositely, the partial agonists may activate D_2Rs in the mesocortical pathway, where low dopamine concentrations prevail (103-105). This concept of functional selectivity motivates further development of partial D_2R agonists as therapeutic "dopamine stabilizers".

In 2000, experimental radioligand binding studies of antipsychotics at the D_2R suggested that atypical antipsychotics dissociate up to 100 times more rapidly as compared to typical antipsychotics; this "fast-off" feature was proposed to facilitate dopamine rebinding at D_2R following drug dissociation, thus preserving the physiological dynamics of dopamine signaling (106). In addition, this hypothesis opposed the theory of 5-HT_2R antagonism reducing the EPS propensity, as D_2R occupancy had the highest correlation with EPS propensity (107). The "fast-off" hypothesis was reinvestigated by analysis of binding kinetics of 17 antagonists at the D_2R, using the Gβγ-mediated GIRK activation assay. Rapid chlorpromazine dissociation from the D_2R and a mere twofold difference in dissociation kinetics between chlorpromazine and clozapine were demonstrated (108), in stark contrast to previous findings by Kapur and Seeman (106). Extended analyses of antipsychotic drug dissociation rates from the D_2R and validation of the GIRK assay results continued to challenge the "fast-off" hypothesis (109), instead proposing the variation in dissociation kinetics and extents of reversibility possibly related to D_2R antagonist lipophilicity (110). A following investigation, using a kinetic assay observing D_2R antagonist competition with the fluorescent D_2R agonist 2-(N-phenethyl-N-propyl)amino-5-hydroxytetralin hydrochloride (PPHT)-red, correlated antipsychotic drug association rates at the D_2R with EPS odds ratios and dissociation rates with the risk of hyperprolactinemia. Pronounced drug-D_2R rebinding due to high association rates, in the context of limited drug diffusion, was proposed to be mechanistically related to a high EPS propensity (111). These findings have been questioned, based on the slow association rate of the used agonist PPHT and the generalization of k_{on} dictating EPS propensities (112). Different determinants of association rates have been suggested, including ligand lipophilicity, diffusion and ligand conformation (113-115).

1.8.3 β-arrestin-biased partial agonists as experimental antipsychotics

The observation that a range of GPCRs were able to affect both canonical G protein, and non-canonical β-arrestin, signaling pathways opened the field of biased signaling (88). Numerous antipsychotic drugs are able to antagonize β-arrestin signaling at the D_2R, in addition to antagonizing G protein signaling (47). A reduction of the β-arrestin downstream effector PKB has been suggested in patients with schizophrenia and the mood stabilizer lithium has been proposed to modulate PKB-GSK3β-signaling (44, 116). At this point, development of β-arrestin-biased ligands opened for further probing of non-canonical GPCR signaling pathways *in vivo*.

In 2011, a series of β-arrestin-selective aripiprazole analogues; UNC9994, UNC9975 and UNC0006, was synthesized at the University of North Carolina, and demonstrated to be devoid of G-protein signaling activity at the D_2R (45). Furthermore, UNC9994 elicited antipsychotic properties in a mouse model of PCP-induced locomotion; this feature was fully reversed in β-arrestin-$2^{-/-}$ mice, supporting the hypothesis that β-arrestin-2-dependent D_2R signaling is involved in mediating antipsychotic drug effects (45). UNC9994 was reported to recruit β-arrestin-2 to D_2R only in the presence of GRK2, especially relevant for cortical tissue with high expression levels of β-arrestin-2 and GRK2 as compared to the striatum, where UNC9994 is an antagonist at β-arrestin-2 D_2R signaling. The resulting cortical β-arrestin-2-selective D_2R agonism increased fast-spiking interneuron activity and was hypothesized to potentially counteract negative symptoms of schizophrenia (117).

2 AIMS OF THE THESIS

The thesis investigates GPCR pharmacology using GIRK current recordings. Specifically, molecular features of ligand binding sites and implications for signaling were explored. Details regarding GPCR-ligand interactions will inform future drug development.

The aims are:

- To determine if the conserved residue $D^{2.50}69$ in the M_2R constitutes a part of the voltage-sensor, mediating voltage-dependent agonist-potency (paper I).

- To determine if the aripiprazole-derived, putatively β-arrestin-selective, D_2R ligand UNC9994 couples to G protein signaling pathways at D_2R and D_3R (paper II).

- To explore binding properties and kinetics of aripiprazole radioanalogues of varying lipophilicity at the D_2R (paper III).

- To experimentally and computationally characterize how a secondary binding pocket in the D_2R may mediate insurmountable ligand binding (paper III).

3 METHODS

3.1 MOLECULAR BIOLOGY

Receptor, accessory protein and ion channel cDNAs were acquired from Genscript (Piscataway, NJ). cDNAs encoding the long-isoform human D_2R (including WT, V91A, L94A and E95A), D_3R and β-arrestin-2 were in the pXOOM vector, which includes the *Xenopus* globin gene (118). All mutations were verified by sequencing. cDNAs encoding RGS4 (from the Missouri cDNA Resource Center; www.cdna.org), GIRK1 and GIRK4 (provided by Dr. Terence Hebert, University of Montreal, Canada) were in pCDNA3 (Invitrogen). cDNAs encoding M_2R (from Dr. Hanna Parnas, Hebrew University of Jerusalem, Israel) and the catalytic subunit of PTX (PTX-S1) were in pGEM-HE. The D69N point mutation was introduced to the WT M_2R using the QuickChange (Agilent technologies) kit according to the manufacturer's instructions. Plasmids were linearized using restriction enzymes (D_2R WT, V91A, L94A and E95A, D_3R, RGS4; XhoI, GIRK1, GIRK4, M_2R WT and D69N; NotI, PTX-S1; NheI) and the DNA product was purified using the PureLink™ kit (Invitrogen; see Fig. 2A). Linearized DNA was transcribed *in vitro* using the mMessage mMachine™ T7 kit (Ambion, Austin, TX). DNA and RNA products were quantified using spectrophotometry (Nanodrop, ThermoFisher).

3.2 *XENOPUS LAEVIS* OOCYTES AS EXPRESSION SYSTEM

Oocytes from the female African clawed toad, *Xenopus laevis*, were surgically isolated according to the procedure described in the ethical permit (N245/15), approved by the Swedish National Board for Laboratory Animals and the Stockholm Ethical Committee. Briefly, the *X. laevis* was immersed for 15 min in 5.4 mM tricaine methanesulfonate (MS-222; Sigma) and 10 mM 4-(2-hydroxyethyl)-1-piperazineethanesulfonic acid (HEPES; Sigma; buffered to pH 7.4 using NaOH). Following verification of anesthesia, a minor laparotomy was performed to allow for extraction of ovarian tissue, which was transferred to a modified Barth's solution (MBS; 88 mM NaCl, 1 mM KCl, 2.4 mM $NaHCO_3$, 15 mM HEPES, 0.33 mM $Ca(NO_3)_2$, 0.41 mM $CaCl_2$ and 0.92 mM $MgSO_4$, 2.5 mM sodium pyruvate, 25 U/ml penicillin and 25 µg/ml streptomycin, buffered to pH 7.6 using NaOH). The abdominal and skin layers were closed separately using 6-0 silk sutures (Ethicon), followed by transfer of the *X. laevis* to a separate tank for observation during the following 24 hours.

Isolated ovarian tissue was treated with 1.5 mg Liberase DH (Roche) for 90 minutes, to separate the individual oocytes, which were subsequently manually screened for adequate staging (stages V-VI (119)) and quality (see Fig. 2A). Oocytes were incubated for 24 hours at 12°C, and thereafter injected with 50 nl of aqueous RNA solution using Nanoject II (Drummond Scientific). The RNA amounts per oocyte were: M_2R (WT), 0.2 ng; M_2R (D69N), 0.7 ng; D_2R (WT, V91A, L94A and E95A), 0.2 ng; D_3R, 0.2 ng; β-arrestin-2, 5.6 ng; PTX-S1, 3 ng; RGS4, 40 ng; GIRK1, GIRK4, 1 ng of each. RGS4 is one of several GAPs

expressed in native tissues, which speed up the G protein cycle such that GIRK channel activity more closely follows receptor occupancy by agonist (120).

3.3 TWO-ELECTRODE VOLTAGE-CLAMP

X. laevis oocytes of maturation stages V-VI have a diameter around 1 mm, substantially larger as compared to neurons or mammalian cell lines. The two-electrode voltage-clamp (TEVC) method allows for precise control of the membrane potential, using separate current-conducting and voltage-following electrodes (121). Activation of GPCRs evoked GIRK currents that were recorded using the TEVC technique (Fig. 2B).

Electrophysiological recordings were performed at room temperature (22°C), 5 to 7 days after RNA injection using the CA-1 amplifier (Dagan, Minneapolis, MN). Data were acquired at 134 Hz using pCLAMP 8 (Molecular Devices) software. A high-potassium solution (64 mM NaCl, 25 mM KCl, 0.8 mM $MgCl_2$, 0.4 mM $CaCl_2$, 15 mM HEPES and 1 mM ascorbic acid, adjusted to pH 7.4 with NaOH), giving a K^+ reversal potential of about -40 mV, was used for GIRK current recordings. Ascorbic acid was added to prevent the oxidation of dopamine. To increase the GIRK currents, oocytes were clamped at -80 mV during registrations. Ligands were added to the 20 µl recording chamber by superfusion at 1.5 ml/min using a computer-controlled, pressure-driven perfusion system (SmartSquirt, AutoMate Scientific, Berkeley, CA).

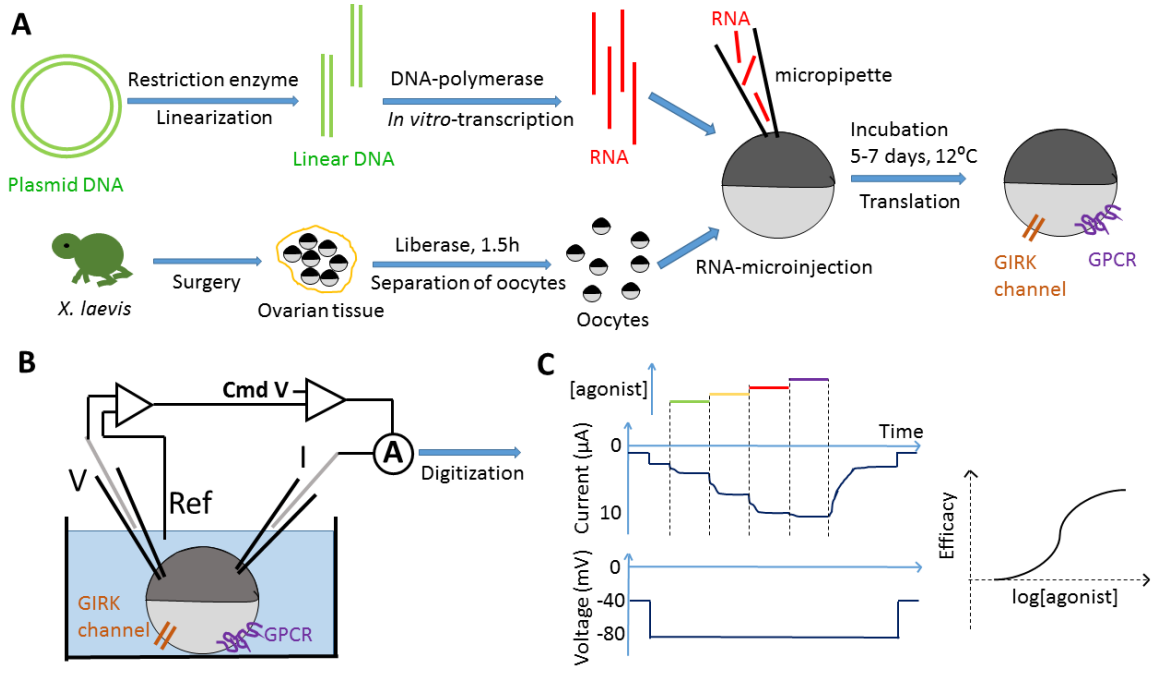

Figure 2. Overview of molecular biology, oocyte preparation, electrophysiology and GIRK recordings. A) Converging pipeline of molecular biology and X. laevis oocyte harvesting, followed by RNA-microinjection and membrane expression of GPCRs and GIRK channels. See Methods 3.1-3.3 for details. B) General principle of two-electrode voltage-clamp of X. laevis oocytes. The voltage-sensing electrode (V) registers the intracellular voltage (by comparison with the bath electrode, Ref), which is compared to the clamped voltage (Cmd V), and if needed a compensatory current is injected into the oocyte via the current-passing electrode (I). The current is registered by an amperometer (A), digitized, and analysed. C) Example of dose-response data, e.g. from oocytes

co-expressing D_2R and GIRK channels. The oocyte is initially clamped to -40 mV and lowered to -80 mV to increase the GIRK currents during the recordings. Increasing agonist concentrations (green-yellow-red-purple) evoke increasing GIRK currents, which saturate around the purple concentration. Following halted agonist administration, the current returns to baseline. The steady-state currents for each concentration may generate dose-response data, here plotted semi-logarithmically. Details are not drawn to scale.

3.4 RECORDING PROTOCOLS

3.4.1 Agonist dose-response curves

For evaluation of agonist ligands, 3 to 4 increasing concentrations were applied at 35-, 50- or 100-second intervals to oocytes expressing the respective receptor (see Fig. 2C). The interval was determined to ensure maximal or pseudomaximal agonism (for ligands demonstrating slow association rates). The agonist-evoked current response was determined by subtracting the basal (agonist-independent) current from the agonist-evoked current. Concentration-responses were subsequently normalized to the mean responses of maximal agonist-evoked responses, either in the same oocytes (expressing D_2R or M_2R; paper I and III) or in other oocytes from the same batch (expressing D_2R and D_3R, the latter desensitizes after agonist application; paper II). For dopamine concentration-response data, 4 to 5 increasing concentrations of dopamine were applied at 25-second intervals, ending with a response-saturating concentration (100 µM) of dopamine.

3.4.2 Antagonist dose-response curves

For dopamine receptor antagonists, 100 nM dopamine was first applied to provide a baseline response, followed by 3 to 4 applications of increasing concentrations of antagonist at 50-100 second intervals in the continued presence of 100 nM dopamine (paper II and III). This allowed for calculation of inhibition constants (K_i) using the Cheng-Prusoff relationship (122). For each oocyte, the current amplitude at the end of each antagonist application interval was normalized to the control response to 100 nM dopamine obtained at the start of the protocol.

3.4.3 Evaluation of ligand binding kinetics

Dissociation rates for acetylcholine (paper I) were determined by fitting a monoexponential function to the decay following agonist washout. Observed association rates (k_{obs}) for antagonists (paper III) were determined by 40 s applications of 100 nM dopamine, followed by varying antagonist concentrations in 100 nM dopamine. A monoexponential function was fitted to the antagonist phase, and the inhibition time constant was converted to k_{obs} (see Methods 3.5.2).

Dissociation rates and extents of recovery for ligands that antagonize the receptor-evoked GIRK channel current (paper III) were determined by application of 1 µM dopamine, followed by ligand in 1 µM DA (antagonizing the response), and subsequent application of either 1 or 100 µM dopamine. Surmountability was defined as an increased agonist response recovery following application of higher agonist concentrations (e.g. 100 µM dopamine vs. 1 µM dopamine).

3.5 DATA ANALYSIS

3.5.1 Dose-response analysis

Electrophysiological data were analyzed in Clampfit (Axon™ Instruments). Dose-response curves were calculated using the variable-slope sigmoidal functions in GraphPad (Prism software). Antagonist data were fitted to the equation:

$$Y = bottom + \frac{1}{1 + 10^{(X - \log_{10} IC_{50})n}}$$

where Y is the response as a fraction of 1, bottom is the maximal response inhibition evoked by the antagonist, X is the logarithm of ligand concentration, IC_{50} is the half maximal inhibitory concentration and n is the Hill slope. For agonist data, the equation used was:

$$Y = \frac{1}{1 + 10^{-(X - \log_{10} EC_{50})n}}$$

where EC_{50} is the half maximal effective concentration of the agonist.

The inhibition constant, K_i, was calculated as

$$K_i = \frac{IC_{50}}{\left(1 + \frac{[agonist]}{EC_{50}}\right)^n}$$

according to Cheng-Prusoff (122). Data points were shown as mean ± SEM.

3.5.2 Estimation of rate constants

GIRK current activation or deactivation kinetics were quantified by fitting a monoexponential decay function

$$q = q_0 + A \times e^{\frac{-(t - t_0)}{\tau}}$$

to data, to estimate the time constant of response decay upon agonist washout. q_0 is the initial and q the final current amplitude, t_0 is the initial and t is the final time point, A is the current amplitude at the start of the fit, and τ is the time constant of current increase or decay.

The association rate constant k_{on} was previously related to the observed association rates, k_{obs}, determined using the GIRK assay (109). Briefly, the calculation is based on a three-state model of agonist-bound receptor (RA), unbound receptor (R) and ligand-bound receptor (RL; see Methods 3.6.1 below), in which the transition between RA and R (agonist dissociation) is assumed to be swift compared to the transition from R to RL (ligand binding). At very high ligand concentrations, a kinetic roof of the k_{obs} may be reached (109) .

By plotting k_{obs} at varying antagonist concentrations, followed by a linear regression, k_{on} was calculated in accordance with previous descriptions (109)

$$k_{on} = \frac{\Delta k_{obs}}{\Delta[antagonist] \times R_0}$$

where the antagonist concentration was known and the fraction of unoccupied receptors, R_0, prior to antagonist application was derived from the dose-response curve of agonist at the relevant receptor. k_{off} was estimated separately as

$$k_{off} = \frac{ln(2)}{T_{1/2}} = \frac{1}{\tau}$$

where ln is the natural logarithm and $T_{1/2}$ is the time for half-maximal response recovery.

Kinetic K_d was calculated as

$$K_d = \frac{k_{off}}{k_{on}}$$

3.5.3 Curve shift assay

For curve shift experiments, a maximal response was first evoked by application of 1 µM dopamine, which was subsequently washed out, followed by the concomitant application of dopamine in the presence (or absence, to generate the control EC_{50}; $EC_{50}C$) of SV-III-130. The current amplitude following 500 s of co-application of dopamine and SV-III-130 was normalized to the initial response elicited by 1 µM dopamine. To extract EC_{50} estimates, normalized responses to the various concentrations of dopamine applied in the presence of each concentration of SV-III-130, or in its absence, were fit by the equation given above to yield $EC_{50}L_z$ or $EC_{50}C$, respectively, where $EC_{50}L_z$ is the EC_{50} in the presence of a given concentration, z, of antagonizing ligand. A Schild plot was generated by plotting; $\log_{10}(EC_{50}L_z/EC_{50}C - 1)$ against SV-III-130 concentration, and linear regression was used to assess the competitiveness of the agonist and ligand interactions. For competitive ligands, the slope is expected to be 1, whereas a ligand with negative allosteric effects typically would demonstrate a slope <1 (123).

3.6 KINETIC BINDING MODELS

Response recovery following D_2R antagonism was simulated based on a three-state model and experimental k_{on} and k_{off} values for ligands and dopamine. For antagonists, k_{on} were derived from k_{obs}, and k_{off} from response recovery experiments using supramaximal dopamine concentrations (100 µM). For dopamine, k_{off} was derived from previous reports using the GIRK assay (124), and k_{on} calculated from the EC_{50} value. k_{on} to irreversibly bound states was calculated for the insurmountable ligand SV-III-130, based on the fraction of response recovery observed after 125 s, assuming that the insurmountable fraction represents the irreversibly bound state.

3.6.1 Three-state competitive binding model

Competitive ligand binding (see e.g. Fig. 1A or C), in the presence of an agonist, was simulated using a three-state model. RA represents agonist-bound receptor, mediating GIRK activation, in the competitive binding model

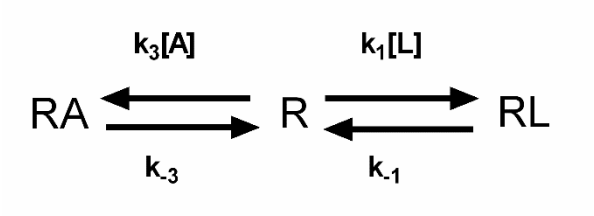

where R, RA and RL denote unbound receptor, agonist-bound receptor and (competing) ligand-bound receptor, k_1, k_{-1}, k_3 and k_{-3}, association and dissociation rate constants for competing ligand and dopamine respectively, L denoting ligand and A agonist (dopamine).

3.6.2 Four-state irreversible binding model of induced-fit type

Irreversible ligand binding was simulated by an induced-fit binding model lacking a dissociation from the second binding step (see e.g. Fig. 1E),

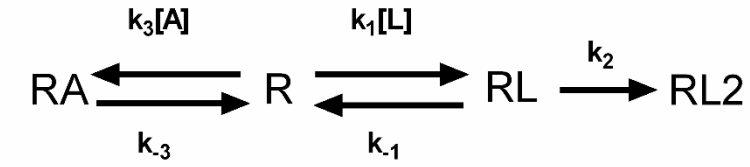

where RL2 denoted the irreversibly bound receptor and k_2 the association rate to the RL2 state. For SV-III-130, k_2 was set to 0.01 s^{-1}, based on the observation that approximately 36% (=1/e) recovery would be observed after 100 s application of 1 µM SV-III-130 in 1 µM DA.

Kinetic binding models were evaluated using Matlab 2018a (MathWorks). The RA fraction, representing the fraction coupled to GIRK channels, was plotted as a function of time (response recovery simulations) or concentration (dose-response simulations).

3.7 MOLECULAR DYNAMICS

Receptor-ligand complexes were generated based on docking of SV-III-130 to the crystal structure of the D_2R (PDB code: 6CM4 (7)). The complexes were placed in a lipid bilayer, with aqueous solution surrounding the membrane and receptor-ligand complex. Using the Accelerating bio-molecular dynamics simulation package (125), the complex was minimized, equilibrated and followed by production runs of 3.2 µs, which were used for analysis. Ligand receptor contacts were quantified using the `get_contacts` script (126). The computed ratio of residue contacts was quantified by dividing the stability of W100 contacts by I184 contacts.

3.8 STATISTICAL ANALYSIS

Current amplitudes, extents of recovery and dissociation half-lives were compared using the Student's t-test. Concentration-response curves were compared using analyses of variance (F-test), to assess differences in pEC_{50}. Observed association rates were plotted against antagonist concentrations, and linear regressions were used to determine the slope and k_{on}. $p<0.05$ was considered significant.

4 RESULTS AND DISCUSSION

4.1 PAPER I

In this study, we investigated the putative voltage-sensing residue in the M_2R by expression of the uncharged D69N mutant and GIRK channels in oocytes. Expression levels of the M_2R D69N allowed for functional characterization of agonist-induced currents at -80 mV and 0 mV using the TEVC technique. The results suggested similar reductions of WT (pEC_{50} = 7.82 ± 0.04 at -80 mV and pEC_{50} = 7.52 ± 0.05 at 0 mV) and D69N receptor potencies (pEC_{50} = 6.80 ± 0.07 at -80 mV and pEC_{50} = 6.47 ± 0.03 at 0 mV) at depolarized potentials, i.e.; a ~2-fold increased EC_{50} at 0 mV compared to -80 mV.

For the M_2R, two prevailing hypotheses regarding voltage-sensing residues have been suggested; either D69 or three tyrosine residues, Y104, Y403 and Y426 (see Introduction, 1.6). Our results contradict previous experimental and computational studies, which have attributed a role to D69 in the voltage-sensing of M_2R and other GPCRs (71, 72, 127). Instead, our results are in agreement with the hypothesis that Y104, Y403 and Y426 are responsible for voltage-dependent agonist potency of the M_2R (73). These findings have implications for understanding the mechanism underlying the depolarization-induced reduction of acetylcholine-evoked GIRK currents in sinoatrial node cardiomyocytes. In the central nervous system, e.g. for dopaminergic projections, the role of voltage-dependent agonist potency and efficacy in regulating presynaptic transmitter release, as well as postsynaptic transmission and neuronal firing patterns, remains largely unexplored.

Reduced M_2R WT and D69N potencies at depolarized potentials were related to increased agonist dissociation rates. Due to small GIRK current amplitudes observed at depolarized potentials for the M_2R D69N, agonist association kinetics were difficult to characterize. The small currents may be related to the pronounced constitutive activity of the M_2R D69N, which reduces the fraction of inactive receptors available to be activated by an agonist. In all, the implications of membrane potential on agonist binding kinetics may provide details regarding which receptor region that is involved in voltage-sensing and inform future studies on voltage-sensing residues in GPCRs.

4.2 PAPER II

In this study, we investigated a potential G protein-coupling of the proposed fully β-arrestin selective D_2R ligand, UNC9994 (45, 117). In oocytes expressing D_2R and GIRK, potent partial agonist efficacy of UNC9994 was observed at D_2R-evoked GIRK currents (pEC_{50} = 6.73±0.4, E_{max} = 14.5±2.8%), indicating G protein-coupled signaling. The partial agonist efficacy of UNC9994 on GIRK activation was abolished by co-expression of PTX-S1 but retained in oocytes co-expressing D_2R and β-arrestin-2. These findings contradict previous investigations (45, 117), where no G protein agonist or antagonist activity of UNC9994 was observed at the D_2R.

UNC9994 demonstrated higher potency and efficacy at the D_3R, eliciting almost full agonism (pEC_{50} = 7.21±0.55, E_{max} = 89.1±24.3%). Possibly, such D_3R interaction may address the proposed beneficial antipsychotic effects of UNC9994 in rodents (45, 117). Interestingly, the D_3R-preferring ligand cariprazine has demonstrated superior efficacy against negative symptoms in patients with schizophrenia as compared to the atypical antipsychotic risperidone, thereby addressing a previously untargeted symptom domain (128).

The suggested binding of UNC9994 at the OBP of the D_2R suggests an ability to compete with dopamine binding (129), and thereby interfering with endogenous activation of G protein signaling pathways. Additionally, the UNC9994 binding mode raises questions regarding the interactions underlying β-arrestin signaling bias. For lysergic acid diethylamide, both the residence time and the β-arrestin signaling efficacy at the $5\text{-}HT_{2A}R$ were reduced following a mutation in the second extracellular loop (ECL2); L209A (130). Structure-functional selectivity-relationship investigations at the D_2R suggested ligand interactions with the ECL2, specifically with I184, over interactions with serine residues of transmembrane helix 5, to bias towards β-arrestin signaling (131). The broader picture of binding kinetics and ligand-receptor interactions governing β-arrestin bias is continuing to be revealed.

4.3 PAPER III

In this study, we investigated a series of aripiprazole (Abilify®) radioanalogues, with varying aliphatic linker lengths that connects the primary and secondary pharmacophores, at the D_2R. SWR-1-8, SV-III-130 and SWR-1-14 have aliphatic linkers of 3, 4 and 5 carbons respectively, with increasing lipophilicity (Fig. 3). Interestingly, SV-III-130 demonstrated potent interactions (pK_i = 8.57±0.05) and an insurmountable binding at the D_2R (fraction of response recovery following antagonism, agonist concentration: 0.20±0.18, 1 µM DA, and 0.23±0.03, 100 µM DA), effects not observed for SWR-1-8 (pK_i = 8.01±0.18, fraction of response recovery following antagonism, agonist concentration: 0.27±0.06, 1 µM DA, and 0.91±0.09, 100 µM DA) or SWR-1-14 (pK_i = 7.70±0.13, fraction of response recovery following antagonism, agonist concentration: 0.37±0.04, 1 µM DA, and 0.98±0.12, 100 µM DA). Thus, the findings are not in agreement with a strict relationship between lipophilicity and insurmountable binding.

The higher potency of SV-III-130 was mediated by both increased association and decreased dissociation rates. Insurmountable binding may be consistent with either a competitive or a non-competitive (e.g. allosteric) binding mechanism. Adaptation of the GIRK activation assay provided curve-shift data of SV-III-130 at varying agonist concentrations. The resulting Schild plot demonstrated a slope close to unity (1.07±0.19, R^2 = 0.97), suggesting a competitive binding mechanism.

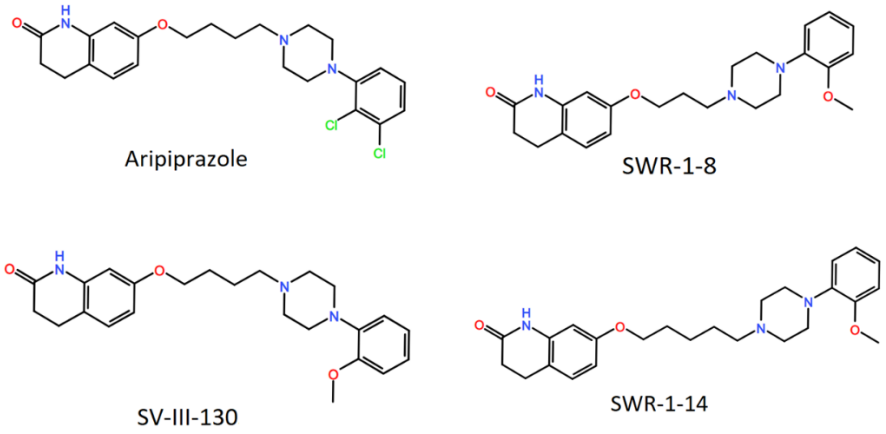

Figure 3. Structures of aripiprazole, SWR-1-8, SV-III-130s and SWR-1-14. Note the shared aliphatic 4 carbon linker in aripiprazole and SV-III-130s. The piperazine moiety constitutes the primary pharmacophore and the tetrahydroquinolinone moiety constitutes the secondary pharmacophore.

The role of the 4 carbon linker was further investigated by alanine mutation of SBP residues V91, L94 and E95, presumed to contact the secondary pharmacophore of SV-III-130 (132). D_2R V91A and E95A reduced the potency (pK_i = 7.63±0.16 for V91A and pK_i = 7.97±0.13 for E95A) and abolished the insurmountability of SV-III-130, whereas the D_2R L94A mutation retained the potency (pK_i = 8.95±0.17 for L94A) and abolished the insurmountability (fraction of response recovery following antagonism, agonist concentration: 0.32±0.05, 1 µM DA, and 0.64±0.11, 100 µM DA). Interestingly, the time to half-maximal response recovery of SV-III-130 from D_2R L94A ($T_{1/2}$ = 107.7±11.4 s, 100 µM DA) resembled that from D_2R WT ($T_{1/2}$ = 110.7±14.8 s, 100 µM DA), although a pronounced surmountability (agonist competition) was observed, suggesting a similar dissociation rate of SV-III-130 from the L94A mutant and from (at least a fraction of) WT D_2R. These findings support a crucial role of V91, L94 and E95 for maintaining the stability of the D_2R SBP and allowing secondary pharmacophore interactions.

To further characterize the competitive, but insurmountable, binding mechanism of SV-III-130 at the D_2R, binding models were adapted based on experimental data (see Methods 3.6 and (9)). A competitive, three-state, ligand-agonist-receptor binding model (109), captured the behavior observed in response recovery experiments with SWR-1-8 and SWR-1-14. Based on the seemingly irreversible binding of SV-III-130 to a fraction of D_2R, as observed during our experimental timescale, two ligand binding steps were included in a second model: First, a reversible step followed by an irreversible one. This four-state model replicated the experimental findings from response recovery experiments with different agonist concentrations. To evaluate the induced-fit binding model of SV-III-130 at the D_2R, an inductive approach was undertaken; prolonged application of SV-III-130 at the D_2R would be expected to extinguish the response recovery, according to the model. In the corresponding experiments, a prolonged (400 s) application of SV-III-130 yielded no response recovery, in

agreement with the model. Additionally, the four-state model replicated the experimental curve-shift assay for SV-III-130 at D_2R WT.

To further investigate the role of L94 in the SBP interaction with the secondary SV-III-130 pharmacophore, molecular dynamics simulations were conducted based on the previously published crystallographic D_2R structure (7). The simulations suggested interactions between the secondary pharmacophore of SV-III-130 and W100 (in the ECL1) and I184 (in the ECL2) of the WT D_2R. Similarly, at the L94A D_2R, the secondary pharmacophore interacted with W100 and I184, although W100 relocated into the cavity previously formed by L94, thereby not sealing the SBP, and possibly increasing the probability of SV-III-130 egress.

The results suggest an insurmountable binding of SV-III-130 at the WT D_2R, which might address the slow and limited displacement of [^{11}C]-SV-III-130 following induced endogenous dopamine release in non-human primates (133). Similarly, the reduced displacement of other D_2R ligands in PET studies may potentially be related to an induced-fit binding mechanism (9). In general, reduced, and slow, drug dissociation could be beneficial in the design of a PET radiotracer or long-acting drug.

Mechanistically, the proposed binding mechanism implies that the primary pharmacophore of SV-III-130 first binds to the OBP and also to the SBP in an open conformation. In the next step, the SBP undergoes a conformational change which closes the extracellular loops 1 and 2 over the ligand through an induced-fit mechanism (9). For ligands with two pharmacophores, a heterobivalent binding mode may be possible (8). However, for SV-III-130, the experimental data on recovery from D_2R antagonism, recorded during a short timeframe (400 s), was recapitulated by an irreversible binding model of induced-fit type. Response recoveries from antagonism by SWR-1-8 and SWR-1-14 were captured by three-state, competitive binding models.

Based on the L94A D_2R mutation, which increased the response recovery following SV-III-130 antagonism, and *in vivo* observations of limited agonist-mediated displacement of [^{11}C]-SV-III-130 (133), an induced-fit binding mechanism was proposed and experimentally tested. Previous descriptions of non-covalent irreversible GPCR-ligand interactions have been described for risperidone at the 5-HT_7R (134, 135).

4.4 LIMITATIONS AND ETHICAL CONSIDERATIONS

Experimentally, papers I-III rely on TEVC investigations of *X. laevis* oocytes, with several shared methodological limitations. Heterologous expression systems demonstrate differences compared to *in vivo* conditions, e.g. in lipid constitution of the cell membrane, co-expression of proteins, post-translational modifications and trafficking mechanisms, and should be regarded as models. The GIRK assay implies that GPCR activation is transmitted to GIRK channels. The coupling efficiency between GPCR and GIRK is increased using a GAP (here RGS4), thereby providing binding and kinetic values in agreement with radioligand binding

studies (109). Batch-dependent variations in GPCR and GIRK expression were reduced whenever possible by normalizing data to the same oocytes, or in some cases (paper II), to oocytes from the same batch. The use of simple kinetic models to explain experimental data (paper III) might not provide a complete picture of the *in vivo* pharmacology, but rather a theoretical model. The explanatory value of such models should be carefully evaluated; for SV-III-130s, we first simulated the expected response recovery following a prolonged SV-III-130 application to D_2R, and thereafter conducted the corresponding experiment.

The use of *X. laevis* oocytes for the present two-electrode voltage-clamp require consideration of the 3Rs; Replacement, Reduction and Refinement (136). Replacement would imply using different biological cells or methods for analysis of receptor-ligand interactions, e.g. assays based on mammalian cell lines. RNA injection of oocytes provides a precise control of stoichiometry and a ground for reproducibility, as compared to corresponding transfections of multiple constructs in mammalian cell lines. Alternative methods may be radioligand binding or fluorometric assays, although these have specific drawbacks with regard to functional measurements and kinetic investigations.

Reduction is fundamental in the use of *X. laevis* oocytes; e.g. by reusing the *X. laevis*. Additionally, multiple experiments should be conducted for each oocyte extraction, to optimize the use of the oocytes. Refinement is conducted by using MS-222, a preferred anesthetic, with analgesic properties (137).

5 CONCLUSIONS

In this thesis, GPCR-ligand interactions in the M_2R and D_2R were explored using electrophysiology and computations.

Voltage-sensing properties of the M_2R were not mediated by $D^{2.50}$ (paper I). Instead, the findings may support the hypothesis of three tyrosine residues (Y104, Y403 and Y426) acting as voltage sensors in the M_2R, as proposed by Barchad-Avitzur et al. (73).

The proposed β-arrestin-selective D_2R ligand, UNC9994, activated GIRK channels via D_2R and D_3R, in a G protein-dependent manner, and in the presence of β-arrestin (paper II). UNC9994 seemed more potent and efficacious at the D_3R, as compared to D_2R. In the light of other investigations suggesting an inability of ligands to evoke β-arrestin signaling without concomitant G protein activation (46), the evidence for completely β-arrestin-selective ligands is currently weak.

The bitopic ligand, SV-III-130, displayed an insurmountable binding at the D_2R (paper III). The two homologues, SWR-1-8 and SWR-1-14 were fully surmountable, which is incongruent with a strict relationship between lipophilicity and insurmountable binding. The competitive binding observed with SV-III-130 at the D_2R was crucially dependent on the integrity of the secondary binding pocket. A two-step, irreversible binding model captured the experimentally observed binding mechanism of SV-III-130. Additionally, molecular dynamics suggested a role of the extracellular loops in modulating SV-III-130 binding to the D_2R.

6 FUTURE DIRECTIONS

GPCR voltage-sensing mechanisms have mainly been investigated in the M_2R. Based on the hypothesis that Y104, Y403 and Y426 act as voltage sensors in the M_2R, the generalizability to other $G\alpha_{i/o}$-coupled GPCRs, e.g. the D_2R, should be considered. Prospective studies investigating inactivating mutations of the corresponding residues in voltage-dependent $G\alpha_{i/o}$-coupled GPCRs, e.g. the D_2R or $mGlu_1R$, would address this hypothesis. Additionally, based on previous findings of agonist-specific voltage-dependency (probe dependence) (68), additional molecular dynamics investigations may provide information regarding the structural network involved in GPCR voltage-sensing.

β-arrestin-selective signaling in the absence of G protein activation remains a controversial but highly interesting topic; ligands with strong β-arrestin preference would allow for the selective study of non-canonical GPCR signaling. Recently, an experimental ligand was reported to be a β-arrestin-selective melatonin 1 receptor agonist, but a mixed G protein/β-arrestin-agonist at the melatonin 2 receptor (136). Further structural-activity relationship investigations of the mechanistic underpinnings of G protein/β-arrestin signaling at various GPCRs will provide insights for the *in silico* development of functionally selective ligands. A truly β-arrestin-selective D_2R ligand would be of substantial value in the research on and development of novel therapeutics for psychotic disorders. Based on the physiological relevance of β-arrestin-biased ligands at several GPCRs, further investigations of receptor-ligand interactions conferring signaling bias is of importance.

Demonstration of induced-fit binding of SV-III-130 at the D_2R indicates that additional ligands could demonstrate similar binding mechanisms. For example, a PET study using the radiotracer [^{18}F]-N-methyl-benperidol reported low displaceability from the D_2R following amphetamine-induced DA competition (138). Based on structural similarities with SV-III-130, N-methyl-benperidol may bind D_2R by an induced-fit binding mechanism. This hypothesis could be addressed using the electrophysiology-based GIRK-assay. Further investigation of bitopic ligands acting at GPCRs may reveal additional induced-fit binding ligands. Also, based on the assumption that the prominent ECL2 of the D_2R is a key mediator in encapsulating the SBP, it would be valuable to investigate whether an induced-fit binding mechanism could be observed at GPCRs with smaller ECL2, e.g. D_3R and D_4R (7). Finally, PET investigations evaluating endogenous dopamine competition with [^{11}C]-SWR-1-8 or [^{11}C]-SWR-1-14 may clarify whether the observed *in vitro* surmountability holds *in vivo*.

7 ACKNOWLEDGEMENTS

This thesis is crucially dependent on the hard work and support of numerous people, to whom I am very thankful. Especially, I wish to express my gratitude to:

Dr. Johanna Nilsson, main supervisor, for giving me the freedom to pursue my own interests in neuroscience.

Professor Peter Århem, co-supervisor, for the endless transmission of scientific knowledge in all possible forms and the interest in computational neuroscience.

Dr. Kristoffer Sahlholm, co-supervisor, for introducing me to electrophysiology, molecular biology and GPCRs.

Dr. Hugo Zeberg, for broad scientific advice, especially regarding theoretical aspects of electrophysiology.

Dr. Jana Selent and Dr. Tomasz Maciej Stępniewski, for productive collaboration and *in silico* contributions.

Dr. Sean W. Reilly, Dr. Robert R. Luedtke and Professor Robert H. Mach, for all work on SWR-1-8, SV-III-130, SWR-1-14, and paper III.

Dr. Matthew Kirkham, for providing theoretical knowledge and practical guidance regarding *X. laevis* husbandry, thereby enabling the research presented above.

The Department of Clinical Neurophysiology, Karolinska University Hospital, for scientific discussions and valuable support.

The administrative staff at the Department of Clinical Neuroscience, for kind helpfulness and physical availability.

All colleagues in Bioclinicum and Biomedicum, Karolinska Institutet, including members of the Svenningsson, Chergui, Holmin, Brundin and Svensson research groups, for interesting discussions, scientific input, collaboration, and for providing a stimulating research environment.

Finally, I wish to express my deepest gratitude to my family and friends for all unconditional and endless support.

8 REFERENCES

1. Lefkowitz RJ, Haber E, Hara D. Identification of the Cardiac Beta-Adrenergic Receptor Protein: Solubilization and Purification by Affinity Chromatography. Proceedings of the National Academy of Sciences. 1972;69(10):2828.

2. Hargrave PA, McDowell JH, Curtis DR, Wang JK, Juszczak E, Fong SL, et al. The structure of bovine rhodopsin. Biophys Struct Mech. 1983;9(4):235-44.

3. Hauser AS, Attwood MM, Rask-Andersen M, Schioth HB, Gloriam DE. Trends in GPCR drug discovery: new agents, targets and indications. Nat Rev Drug Discov. 2017;16(12):829-42.

4. Olten B, Bloch MH. Meta regression: Relationship between antipsychotic receptor binding profiles and side-effects. Prog Neuropsychopharmacol Biol Psychiatry. 2018;84(Pt A):272-81.

5. Kaupmann K, Malitschek B, Schuler V, Heid J, Froestl W, Beck P, et al. GABA(B)-receptor subtypes assemble into functional heteromeric complexes. Nature. 1998;396(6712):683-7.

6. Gomes I, Ayoub MA, Fujita W, Jaeger WC, Pfleger KDG, Devi LA. G Protein-Coupled Receptor Heteromers. Annual review of pharmacology and toxicology. 2016;56:403-25.

7. Wang S, Che T, Levit A, Shoichet BK, Wacker D, Roth BL. Structure of the D2 dopamine receptor bound to the atypical antipsychotic drug risperidone. Nature. 2018;555(7695):269-73.

8. Vauquelin G, Hall D, Charlton SJ. 'Partial' competition of heterobivalent ligand binding may be mistaken for allosteric interactions: a comparison of different target interaction models. British Journal of Pharmacology. 2015;172(9):2300-15.

9. Vauquelin G, Van Liefde I, Swinney DC. On the different experimental manifestations of two-state 'induced-fit' binding of drugs to their cellular targets. Br J Pharmacol. 2016;173(8):1268-85.

10. Copeland RA. The drug–target residence time model: a 10-year retrospective. Nature Reviews Drug Discovery. 2016;15(2):87-95.

11. Meltzer HY, Massey BW. The role of serotonin receptors in the action of atypical antipsychotic drugs. Curr Opin Pharmacol. 2011;11(1):59-67.

12. Abila B, Wilson JF, Marshall RW, Richens A. The tremorolytic action of beta-adrenoceptor blockers in essential, physiological and isoprenaline-induced tremor is mediated by beta-adrenoceptors located in a deep peripheral compartment. Br J Clin Pharmacol. 1985;20(4):369-76.

13. Baker JG, Hall IP, Hill SJ. Agonist and inverse agonist actions of beta-blockers at the human beta 2-adrenoceptor provide evidence for agonist-directed signaling. Mol Pharmacol. 2003;64(6):1357-69.

14. Kenakin T. New concepts in drug discovery: collateral efficacy and permissive antagonism. Nat Rev Drug Discov. 2005;4(11):919-27.

15. Ehlert FJ. Analysis of allosterism in functional assays. J Pharmacol Exp Ther. 2005;315(2):740-54.

16. Urwyler S, Mosbacher J, Lingenhoehl K, Heid J, Hofstetter K, Froestl W, et al. Positive allosteric modulation of native and recombinant gamma-aminobutyric acid(B) receptors by 2,6-Di-tert-butyl-4-(3-hydroxy-2,2-dimethyl-propyl)-phenol (CGP7930) and its aldehyde analog CGP13501. Mol Pharmacol. 2001;60(5):963-71.

17. Wold EA, Chen J, Cunningham KA, Zhou J. Allosteric Modulation of Class A GPCRs: Targets, Agents, and Emerging Concepts. J Med Chem. 2019;62(1):88-127.

18. Masuho I, Ostrovskaya O, Kramer GM, Jones CD, Xie K, Martemyanov KA. Distinct profiles of functional discrimination among G proteins determine the actions of G protein-coupled receptors. Sci Signal. 2015;8(405):ra123.

19. DeWire SM, Yamashita DS, Rominger DH, Liu G, Cowan CL, Graczyk TM, et al. A G Protein-Biased Ligand at the μ-Opioid Receptor Is Potently Analgesic with Reduced Gastrointestinal and Respiratory Dysfunction Compared with Morphine. Journal of Pharmacology and Experimental Therapeutics. 2013;344(3):708.

20. McCudden CR, Hains MD, Kimple RJ, Siderovski DP, Willard FS. G-protein signaling: back to the future. Cellular and molecular life sciences : CMLS. 2005;62(5):551-77.

21. Frank M, Thumer L, Lohse MJ, Bunemann M. G Protein activation without subunit dissociation depends on a G{alpha}(i)-specific region. J Biol Chem. 2005;280(26):24584-90.

22. Gill DM, Meren R. ADP-ribosylation of membrane proteins catalyzed by cholera toxin: basis of the activation of adenylate cyclase. Proc Natl Acad Sci U S A. 1978;75(7):3050-4.

23. Cassel D, Pfeuffer T. Mechanism of cholera toxin action: covalent modification of the guanyl nucleotide-binding protein of the adenylate cyclase system. Proc Natl Acad Sci U S A. 1978;75(6):2669-73.

24. Bokoch GM, Katada T, Northup JK, Hewlett EL, Gilman AG. Identification of the predominant substrate for ADP-ribosylation by islet activating protein. J Biol Chem. 1983;258(4):2072-5.

25. Codina J, Hildebrandt J, Iyengar R, Birnbaumer L, Sekura RD, Manclark CR. Pertussis toxin substrate, the putative Ni component of adenylyl cyclases, is an alpha beta heterodimer regulated by guanine nucleotide and magnesium. Proc Natl Acad Sci U S A. 1983;80(14):4276-80.

26. Biel M, Michalakis S. Cyclic nucleotide-gated channels. Handb Exp Pharmacol. 2009(191):111-36.

27. Wolfe JT, Wang H, Howard J, Garrison JC, Barrett PQ. T-type calcium channel regulation by specific G-protein betagamma subunits. Nature. 2003;424(6945):209-13.

28. Kleuss C, Scherubl H, Hescheler J, Schultz G, Wittig B. Selectivity in signal transduction determined by gamma subunits of heterotrimeric G proteins. Science. 1993;259(5096):832-4.

29. Wickman K, Karschin C, Karschin A, Picciotto MR, Clapham DE. Brain localization and behavioral impact of the G-protein-gated K+ channel subunit GIRK4. J Neurosci. 2000;20(15):5608-15.

30. Lüscher C, Slesinger PA. Emerging roles for G protein-gated inwardly rectifying potassium (GIRK) channels in health and disease. Nature reviews Neuroscience. 2010;11(5):301-15.

31. Lesage F, Guillemare E, Fink M, Duprat F, Heurteaux C, Fosset M, et al. Molecular properties of neuronal G-protein-activated inwardly rectifying K+ channels. J Biol Chem. 1995;270(48):28660-7.

32. Huang CL, Feng S, Hilgemann DW. Direct activation of inward rectifier potassium channels by PIP2 and its stabilization by Gbetagamma. Nature. 1998;391(6669):803-6.

33. Ho IH, Murrell-Lagnado RD. Molecular determinants for sodium-dependent activation of G protein-gated K+ channels. J Biol Chem. 1999;274(13):8639-48.

34. Whorton MR, MacKinnon R. Crystal structure of the mammalian GIRK2 K+ channel and gating regulation by G proteins, PIP2, and sodium. Cell. 2011;147(1):199-208.

35. Touhara KK, MacKinnon R. Molecular basis of signaling specificity between GIRK channels and GPCRs. eLife. 2018;7:e42908.

36. Jaen C, Doupnik CA. RGS3 and RGS4 differentially associate with G protein-coupled receptor-Kir3 channel signaling complexes revealing two modes of RGS modulation. Precoupling and collision coupling. J Biol Chem. 2006;281(45):34549-60.

37. Wang D, Tan YC, Kreitzer GE, Nakai Y, Shan D, Zheng Y, et al. G proteins G12 and G13 control the dynamic turnover of growth factor-induced dorsal ruffles. J Biol Chem. 2006;281(43):32660-7.

38. Ribas C, Penela P, Murga C, Salcedo A, García-Hoz C, Jurado-Pueyo M, et al. The G protein-coupled receptor kinase (GRK) interactome: Role of GRKs in GPCR regulation and signaling. Biochimica et Biophysica Acta (BBA) - Biomembranes. 2007;1768(4):913-22.

39. Lefkowitz RJ, Shenoy SK. Transduction of receptor signals by beta-arrestins. Science. 2005;308(5721):512-7.

40. Albensi BC, Mattson MP. Evidence for the involvement of TNF and NF-kappaB in hippocampal synaptic plasticity. Synapse. 2000;35(2):151-9.

41. Wang DB, Kinoshita C, Kinoshita Y, Morrison RS. p53 and mitochondrial function in neurons. Biochimica et biophysica acta. 2014;1842(8):1186-97.

42. Ebisuya M, Kondoh K, Nishida E. The duration, magnitude and compartmentalization of ERK MAP kinase activity: mechanisms for providing signaling specificity. J Cell Sci. 2005;118(Pt 14):2997-3002.

43. Shenoy SK, Drake MT, Nelson CD, Houtz DA, Xiao K, Madabushi S, et al. beta-arrestin-dependent, G protein-independent ERK1/2 activation by the beta2 adrenergic receptor. J Biol Chem. 2006;281(2):1261-73.

44. Beaulieu JM, Marion S, Rodriguiz RM, Medvedev IO, Sotnikova TD, Ghisi V, et al. A beta-arrestin 2 signaling complex mediates lithium action on behavior. Cell. 2008;132(1):125-36.

45. Allen JA, Yost JM, Setola V, Chen X, Sassano MF, Chen M, et al. Discovery of β-Arrestin–Biased Dopamine D₂ Ligands for Probing Signal Transduction Pathways Essential for Antipsychotic Efficacy. Proceedings of the National Academy of Sciences. 2011;108(45):18488.

46. Grundmann M, Merten N, Malfacini D, Inoue A, Preis P, Simon K, et al. Lack of beta-arrestin signaling in the absence of active G proteins. Nat Commun. 2018;9(1):341.

47. Masri B, Salahpour A, Didriksen M, Ghisi V, Beaulieu JM, Gainetdinov RR, et al. Antagonism of dopamine D2 receptor/beta-arrestin 2 interaction is a common property of clinically effective antipsychotics. Proc Natl Acad Sci U S A. 2008;105(36):13656-61.

48. Hodavance SY, Gareri C, Torok RD, Rockman HA. G Protein-coupled Receptor Biased Agonism. J Cardiovasc Pharmacol. 2016;67(3):193-202.

49. Kruse AC, Weiss DR, Rossi M, Hu J, Hu K, Eitel K, et al. Muscarinic receptors as model targets and antitargets for structure-based ligand discovery. Molecular pharmacology. 2013;84(4):528-40.

50. Scarr E. Muscarinic receptors: their roles in disorders of the central nervous system and potential as therapeutic targets. CNS Neurosci Ther. 2012;18(5):369-79.

51. Gerber DJ, Sotnikova TD, Gainetdinov RR, Huang SY, Caron MG, Tonegawa S. Hyperactivity, elevated dopaminergic transmission, and response to amphetamine in M1 muscarinic acetylcholine receptor-deficient mice. Proc Natl Acad Sci U S A. 2001;98(26):15312-7.

52. Bymaster FP, Carter PA, Yamada M, Gomeza J, Wess J, Hamilton SE, et al. Role of specific muscarinic receptor subtypes in cholinergic parasympathomimetic responses, in vivo phosphoinositide hydrolysis, and pilocarpine-induced seizure activity. Eur J Neurosci. 2003;17(7):1403-10.

53. Hibino H, Inanobe A, Furutani K, Murakami S, Findlay I, Kurachi Y. Inwardly rectifying potassium channels: their structure, function, and physiological roles. Physiol Rev. 2010;90(1):291-366.

54. Moehle MS, Conn PJ. Roles of the M4 acetylcholine receptor in the basal ganglia and the treatment of movement disorders. Mov Disord. 2019;34(8):1089-99.

55. Ztaou S, Maurice N, Camon J, Guiraudie-Capraz G, Kerkerian-Le Goff L, Beurrier C, et al. Involvement of Striatal Cholinergic Interneurons and M1 and M4 Muscarinic Receptors in Motor Symptoms of Parkinson's Disease. J Neurosci. 2016;36(35):9161-72.

56. Basile AS, Fedorova I, Zapata A, Liu X, Shippenberg T, Duttaroy A, et al. Deletion of the M₅ muscarinic acetylcholine receptor attenuates morphine reinforcement and withdrawal but not morphine analgesia. Proceedings of the National Academy of Sciences. 2002;99(17):11452.

57. Thal DM, Sun B, Feng D, Nawaratne V, Leach K, Felder CC, et al. Crystal structures of the M1 and M4 muscarinic acetylcholine receptors. Nature. 2016;531(7594):335-40.

58. Kruse AC, Ring AM, Manglik A, Hu J, Hu K, Eitel K, et al. Activation and allosteric modulation of a muscarinic acetylcholine receptor. Nature. 2013;504(7478):101-6.

59. Kruse AC, Hu J, Pan AC, Arlow DH, Rosenbaum DM, Rosemond E, et al. Structure and dynamics of the M3 muscarinic acetylcholine receptor. Nature. 2012;482(7386):552-6.

60. Vuckovic Z, Gentry PR, Berizzi AE, Hirata K, Varghese S, Thompson G, et al. Crystal structure of the M₅ muscarinic acetylcholine receptor. Proceedings of the National Academy of Sciences. 2019;116(51):26001.

61. Magleby KL, Stevens CF. The effect of voltage on the time course of end-plate currents. J Physiol. 1972;223(1):151-71.

62. Ben-Chaim Y, Tour O, Dascal N, Parnas I, Parnas H. The M2 muscarinic G-protein-coupled receptor is voltage-sensitive. J Biol Chem. 2003;278(25):22482-91.

63. Ohana L, Barchad O, Parnas I, Parnas H. The metabotropic glutamate G-protein-coupled receptors mGluR3 and mGluR1a are voltage-sensitive. J Biol Chem. 2006;281(34):24204-15.

64. Ben-Chaim Y, Chanda B, Dascal N, Bezanilla F, Parnas I, Parnas H. Movement of 'gating charge' is coupled to ligand binding in a G-protein-coupled receptor. Nature. 2006;444(7115):106-9.

65. Sahlholm K, Nilsson J, Marcellino D, Fuxe K, Arhem P. The human histamine H3 receptor couples to GIRK channels in Xenopus oocytes. Eur J Pharmacol. 2007;567(3):206-10.

66. Sahlholm K, Nilsson J, Marcellino D, Fuxe K, Arhem P. Electrophysiology-based analysis of human histamine H(4) receptor pharmacology using GIRK channel coupling in Xenopus oocytes. Eur J Pharmacol. 2008;591(1-3):52-8.

67. Sahlholm K, Nilsson J, Marcellino D, Fuxe K, Arhem P. Voltage-dependence of the human dopamine D2 receptor. Synapse. 2008;62(6):476-80.

68. Sahlholm K, Barchad-Avitzur O, Marcellino D, Gomez-Soler M, Fuxe K, Ciruela F, et al. Agonist-specific voltage sensitivity at the dopamine D2S receptor--molecular determinants and relevance to therapeutic ligands. Neuropharmacology. 2011;61(5-6):937-49.

69. Ballesteros JA, Weinstein H. [19] Integrated methods for the construction of three-dimensional models and computational probing of structure-function relations in G protein-coupled receptors. In: Sealfon SC, editor. Methods in Neurosciences: Academic Press; 1995. p. 366-428.

70. Katritch V, Fenalti G, Abola EE, Roth BL, Cherezov V, Stevens RC. Allosteric sodium in class A GPCR signaling. Trends Biochem Sci. 2014;39(5):233-44.

71. Navarro-Polanco RA, Moreno Galindo EG, Ferrer-Villada T, Arias M, Rigby JR, Sanchez-Chapula JA, et al. Conformational changes in the M2 muscarinic receptor induced by membrane voltage and agonist binding. J Physiol. 2011;589(Pt 7):1741-53.

72. Vickery ON, Machtens JP, Zachariae U. Membrane potentials regulating GPCRs: insights from experiments and molecular dynamics simulations. Curr Opin Pharmacol. 2016;30:44-50.

73. Barchad-Avitzur O, Priest MF, Dekel N, Bezanilla F, Parnas H, Ben-Chaim Y. A Novel Voltage Sensor in the Orthosteric Binding Site of the M2 Muscarinic Receptor. Biophys J. 2016;111(7):1396-408.

74. Noma A, Trautwein W. Relaxation of the ACh-induced potassium current in the rabbit sinoatrial node cell. Pflugers Arch. 1978;377(3):193-200.

75. Moreno-Galindo EG, Sanchez-Chapula JA, Sachse FB, Rodriguez-Paredes JA, Tristani-Firouzi M, Navarro-Polanco RA. Relaxation gating of the acetylcholine-activated inward rectifier K+ current is mediated by intrinsic voltage sensitivity of the muscarinic receptor. J Physiol. 2011;589(Pt 7):1755-67.

76. Björklund A, Dunnett SB. Fifty years of dopamine research. Elsevier; 2007.

77. Jaber M, Robinson SW, Missale C, Caron MG. Dopamine receptors and brain function. Neuropharmacology. 1996;35(11):1503-19.

78. El-Ghundi M, O'Dowd BF, George SR. Insights into the role of dopamine receptor systems in learning and memory. Rev Neurosci. 2007;18(1):37-66.

79. Andersen PH, Gingrich JA, Bates MD, Dearry A, Falardeau P, Senogles SE, et al. Dopamine receptor subtypes: beyond the D1/D2 classification. Trends Pharmacol Sci. 1990;11(6):231-6.

80. Hall H, Sedvall G, Magnusson O, Kopp J, Halldin C, Farde L. Distribution of D1- and D2-Dopamine Receptors, and Dopamine and Its Metabolites in the Human Brain. Neuropsychopharmacology. 2003;11:245.

81. Goldman-Rakic PS, Castner SA, Svensson TH, Siever LJ, Williams GV. Targeting the dopamine D1 receptor in schizophrenia: insights for cognitive dysfunction. Psychopharmacology (Berl). 2004;174(1):3-16.

82. McNab F, Varrone A, Farde L, Jucaite A, Bystritsky P, Forssberg H, et al. Changes in cortical dopamine D1 receptor binding associated with cognitive training. Science. 2009;323(5915):800-2.

83. Russo SJ, Nestler EJ. The brain reward circuitry in mood disorders. Nat Rev Neurosci. 2013;14(9):609-25.

84. Hasbi A, O'Dowd BF, George SR. Dopamine D1-D2 receptor heteromer signaling pathway in the brain: emerging physiological relevance. Molecular brain. 2011;4:26-.

85. Scarselli M, Novi F, Schallmach E, Lin R, Baragli A, Colzi A, et al. D2/D3 dopamine receptor heterodimers exhibit unique functional properties. J Biol Chem. 2001;276(32):30308-14.

86. Wang S, Wacker D, Levit A, Che T, Betz RM, McCorvy JD, et al. D4 dopamine receptor high-resolution structures enable the discovery of selective agonists. Science. 2017;358(6361):381-6.

87. Chien EY, Liu W, Zhao Q, Katritch V, Han GW, Hanson MA, et al. Structure of the human dopamine D3 receptor in complex with a D2/D3 selective antagonist. Science. 2010;330(6007):1091-5.

88. Beaulieu JM, Gainetdinov RR. The physiology, signaling, and pharmacology of dopamine receptors. Pharmacol Rev. 2011;63(1):182-217.

89. Fearnley JM, Lees AJ. Ageing and Parkinson's disease: substantia nigra regional selectivity. Brain. 1991;114 (Pt 5):2283-301.

90. Damier P, Hirsch EC, Agid Y, Graybiel AM. The substantia nigra of the human brain. II. Patterns of loss of dopamine-containing neurons in Parkinson's disease. Brain. 1999;122 (Pt 8):1437-48.

91. Bird ED, Spokes EGS, Iversen LL. DOPAMINE AND NORADRENALINE IN POST-MORTEM BRAIN IN HUNTINGTON'S DISEASE AND SCHIZOPHRENIC ILLNESS. Acta Psychiatr Scand. 1980;61(S280):63-73.

92. Howes OD, Kapur S. The dopamine hypothesis of schizophrenia: version III--the final common pathway. Schizophr Bull. 2009;35(3):549-62.

93. Abi-Dargham A, Rodenhiser J, Printz D, Zea-Ponce Y, Gil R, Kegeles LS, et al. Increased baseline occupancy of D2 receptors by dopamine in schizophrenia. Proc Natl Acad Sci U S A. 2000;97(14):8104-9.

94. Cousins DA, Butts K, Young AH. The role of dopamine in bipolar disorder. Bipolar Disord. 2009;11(8):787-806.

95. Davis KL, Kahn RS, Ko G, Davidson M. Dopamine in schizophrenia: a review and reconceptualization. Am J Psychiatry. 1991;148(11):1474-86.

96. Howes OD, Kapur S. The dopamine hypothesis of schizophrenia: version III--the final common pathway. Schizophrenia bulletin. 2009;35(3):549-62.

97. Coyle JT. The glutamatergic dysfunction hypothesis for schizophrenia. Harv Rev Psychiatry. 1996;3(5):241-53.

98. Erhardt S, Schwieler L, Imbeault S, Engberg G. The kynurenine pathway in schizophrenia and bipolar disorder. Neuropharmacology. 2017;112(Pt B):297-306.

99. Weiden PJ. EPS profiles: the atypical antipsychotics are not all the same. J Psychiatr Pract. 2007;13(1):13-24.

100. Farde L, Nordstrom AL, Wiesel FA, Pauli S, Halldin C, Sedvall G. Positron emission tomographic analysis of central D1 and D2 dopamine receptor occupancy in patients treated with classical neuroleptics and clozapine. Relation to extrapyramidal side effects. Arch Gen Psychiatry. 1992;49(7):538-44.

101. Kapur S. 5-HT2 antagonism and EPS benefits: is there a causal connection? Psychopharmacology (Berl). 1996;124(1-2):35-9.

102. Tyrer P, Kendall T. The spurious advance of antipsychotic drug therapy. Lancet. 2009;373(9657):4-5.

103. Mailman RB, Murthy V. Third generation antipsychotic drugs: partial agonism or receptor functional selectivity? Current pharmaceutical design. 2010;16(5):488-501.

104. Lieberman JA. Dopamine partial agonists: a new class of antipsychotic. CNS Drugs. 2004;18(4):251-67.

105. Urban JD, Clarke WP, von Zastrow M, Nichols DE, Kobilka B, Weinstein H, et al. Functional selectivity and classical concepts of quantitative pharmacology. J Pharmacol Exp Ther. 2007;320(1):1-13.

106. Kapur S, Seeman P. Antipsychotic agents differ in how fast they come off the dopamine D2 receptors. Implications for atypical antipsychotic action. J Psychiatry Neurosci. 2000;25(2):161-6.

107. Kapur S, Seeman P. Does fast dissociation from the dopamine d(2) receptor explain the action of atypical antipsychotics?: A new hypothesis. Am J Psychiatry. 2001;158(3):360-9.

108. Sahlholm K, Marcellino D, Nilsson J, Ogren SO, Fuxe K, Arhem P. Typical and atypical antipsychotics do not differ markedly in their reversibility of antagonism of the dopamine D2 receptor. Int J Neuropsychopharmacol. 2014;17(1):149-55.

109. Sahlholm K, Zeberg H, Nilsson J, Ogren SO, Fuxe K, Arhem P. The fast-off hypothesis revisited: A functional kinetic study of antipsychotic antagonism of the dopamine D2 receptor. Eur Neuropsychopharmacol. 2016;26(3):467-76.

110. Vauquelin G, Bostoen S, Vanderheyden P, Seeman P. Clozapine, atypical antipsychotics, and the benefits of fast-off D2 dopamine receptor antagonism. Naunyn Schmiedebergs Arch Pharmacol. 2012;385(4):337-72.

111. Sykes DA, Moore H, Stott L, Holliday N, Javitch JA, Lane JR, et al. Extrapyramidal side effects of antipsychotics are linked to their association kinetics at dopamine D2 receptors. Nature Communications. 2017;8(1):763.

112. Zeberg H, Sahlholm K. Antipsychotics with similar association kinetics at dopamine D2 receptors differ in extrapyramidal side-effects. Nature Communications. 2018;9(1):3577.

113. Pan AC, Borhani DW, Dror RO, Shaw DE. Molecular determinants of drug-receptor binding kinetics. Drug Discov Today. 2013;18(13-14):667-73.

114. Sykes DA, Stoddart LA, Kilpatrick LE, Hill SJ. Binding kinetics of ligands acting at GPCRs. Molecular and cellular endocrinology. 2019;485:9-19.

115. Sykes DA, Parry C, Reilly J, Wright P, Fairhurst RA, Charlton SJ. Observed drug-receptor association rates are governed by membrane affinity: the importance of establishing "micro-pharmacokinetic/pharmacodynamic relationships" at the beta2-adrenoceptor. Mol Pharmacol. 2014;85(4):608-17.

116. Emamian ES, Hall D, Birnbaum MJ, Karayiorgou M, Gogos JA. Convergent evidence for impaired AKT1-GSK3beta signaling in schizophrenia. Nat Genet. 2004;36(2):131-7.

117. Urs NM, Gee SM, Pack TF, McCorvy JD, Evron T, Snyder JC, et al. Distinct cortical and striatal actions of a β-arrestin–biased dopamine D2 receptor ligand reveal unique antipsychotic-like properties. Proceedings of the National Academy of Sciences. 2016.

118. Jespersen T, Grunnet M, Angelo K, Klaerke DA, Olesen SP. Dual-function vector for protein expression in both mammalian cells and Xenopus laevis oocytes. Biotechniques. 2002;32(3):536-8, 40.

119. Dumont JN. Oogenesis in Xenopus laevis (Daudin). I. Stages of oocyte development in laboratory maintained animals. J Morphol. 1972;136(2):153-79.

120. Dascal N, Kahanovitch U. The Roles of Gbetagamma and Galpha in Gating and Regulation of GIRK Channels. Int Rev Neurobiol. 2015;123:27-85.

121. Guan B, Chen X, Zhang H. Two-electrode voltage clamp. Methods Mol Biol. 2013;998:79-89.

122. Cheng Y, Prusoff WH. Relationship between the inhibition constant (K1) and the concentration of inhibitor which causes 50 per cent inhibition (I50) of an enzymatic reaction. Biochem Pharmacol. 1973;22(23):3099-108.

123. Christopoulos A, Kenakin T. G protein-coupled receptor allosterism and complexing. Pharmacol Rev. 2002;54(2):323-74.

124. Sahlholm K. The role of RGS protein in agonist-dependent relaxation of GIRK currents in Xenopus oocytes. Biochem Biophys Res Commun. 2011;415(3):509-14.

125. Harvey MJ, Giupponi G, Fabritiis GD. ACEMD: Accelerating Biomolecular Dynamics in the Microsecond Time Scale. J Chem Theory Comput. 2009;5(6):1632-9.

126. Venkatakrishnan AJ, Fonseca R, Ma AK, Hollingsworth SA, Chemparathy A, Hilger D, et al. Uncovering patterns of atomic interactions in static and dynamic structures of proteins. bioRxiv. 2019:840694.

127. Vickery ON, Machtens JP, Tamburrino G, Seeliger D, Zachariae U. Structural Mechanisms of Voltage Sensing in G Protein-Coupled Receptors. Structure. 2016;24(6):997-1007.

128. Németh G, Laszlovszky I, Czobor P, Szalai E, Szatmári B, Harsányi J, et al. Cariprazine versus risperidone monotherapy for treatment of predominant negative symptoms in patients with schizophrenia: a randomised, double-blind, controlled trial. The Lancet. 2017;389(10074):1103-13.

129. Lane JR, Chubukov P, Liu W, Canals M, Cherezov V, Abagyan R, et al. Structure-based ligand discovery targeting orthosteric and allosteric pockets of dopamine receptors. Molecular pharmacology. 2013;84(6):794-807.

130. Wacker D, Wang S, McCorvy JD, Betz RM, Venkatakrishnan AJ, Levit A, et al. Crystal Structure of an LSD-Bound Human Serotonin Receptor. Cell. 2017;168(3):377-89.e12.

131. McCorvy JD, Butler KV, Kelly B, Rechsteiner K, Karpiak J, Betz RM, et al. Structure-inspired design of beta-arrestin-biased ligands for aminergic GPCRs. Nat Chem Biol. 2018;14(2):126-34.

132. Luedtke RR, Mishra Y, Wang Q, Griffin SA, Bell-Horner C, Taylor M, et al. Comparison of the binding and functional properties of two structurally different D2 dopamine receptor subtype selective compounds. ACS chemical neuroscience. 2012;3(12):1050-62.

133. Xu J, Vangveravong S, Li S, Fan J, Jones LA, Cui J, et al. Positron emission tomography imaging of dopamine D2 receptors using a highly selective radiolabeled D2 receptor partial agonist. Neuroimage. 2013;71:168-74.

134. Teitler M, Toohey N, Knight JA, Klein MT, Smith C. Clozapine and other competitive antagonists reactivate risperidone-inactivated h5-HT7 receptors: radioligand binding and functional evidence for GPCR homodimer protomer interactions. Psychopharmacology. 2010;212(4):687-97.

135. Smith C, Rahman T, Toohey N, Mazurkiewicz J, Herrick-Davis K, Teitler M. Risperidone irreversibly binds to and inactivates the h5-HT7 serotonin receptor. Mol Pharmacol. 2006;70(4):1264-70.

136. Patel N, Huang XP, Grandner JM, Johansson LC, Stauch B, McCorvy JD, et al. Structure-based discovery of potent and selective melatonin receptor agonists. Elife. 2020;9.

137. Guenette SA, Giroux MC, Vachon P. Pain perception and anaesthesia in research frogs. Exp Anim. 2013;62(2):87-92.

138. Moerlein SM, Perlmutter JS, Markham J, Welch MJ. In Vivo Kinetics of [18F](N-Methyl)Benperidol: A Novel PET Tracer for Assessment of Dopaminergic D2-Like Receptor Binding. Journal of Cerebral Blood Flow & Metabolism. 1997;17(8):833-45.